

Thermal transport in antiferromagnetic spin-chain materials

A. L. Chernyshev¹ and A. V. Rozhkov²

¹*Department of Physics, University of California, Irvine, California 92697*

²*Institute for Theoretical and Applied Electrodynamics IIHT RAS,
Moscow, ul. Izhorskaya 13/19, 127412, Russian Federation*

(Dated: February 2, 2008)

We study the problem of heat transport in one-dimensional (1D) spin-chain systems weakly coupled to three-dimensional phonons and impurities. We consider the limit of fast spin excitations and slow phonons, applicable to a number of compounds of the cuprates family, such as Sr_2CuO_3 , where the superexchange J is much larger than the Debye energy, Θ_D . In this case the Umklapp scattering among the spin excitations is strongly suppressed for all relevant temperatures. We argue that the leading scattering mechanism for the spin excitations at not too low temperatures is the “normal” (as opposed to the Umklapp) spin-phonon scattering in which the non-equilibrium momentum is transferred from the spin subsystem to phonons where it quickly relaxes through the “phonon bath”. Because of the lower dimensionality of the spin excitations it is only the momentum along the chains which is conserved in such a scattering. We find that this effect leads to a particular momentum- and temperature-dependence of the spin-phonon relaxation rate valid for the broad class of low-dimensional spin systems. Subsequently we demonstrate that the spin-phonon relaxation mechanism is insufficient for the low-energy, long-wavelength 1D spin-chain excitations, which make the thermal conductivity diverge. We complete our consideration by taking into account the impurity scattering, which in 1D cuts off the quasi-ballistic spin excitations and renders the thermal conductivity finite. Altogether, these effects yield the following spin-boson thermal conductivity behavior: $\kappa_s \propto T^2$ at low temperatures, $\kappa_s \propto T^{-1}$ at intermediate temperatures, and $\kappa_s = \text{const}$ at higher temperatures $T \sim \Theta_D$. The saturation at higher temperatures is of rather non-trivial origin and we provide a detailed discussion of it. Our results compare very well with the existing experimental data for Sr_2CuO_3 . Using our microscopic insight into the problem we propose further experiments and predict an unusual impurity concentration dependence for a number of quantities.

PACS numbers: 75.10.Pq, 71.10.Pm, 72.10.Bg, 75.40.Gb

I. INTRODUCTION

Experiments. Recent experiments in low-dimensional quantum magnets^{1,2,3,4,5,6,7,8,9,10,11,12,13,14,15,16,17,18} have revealed remarkably strong thermal transport anomalies associated with the low-dimensional spin degrees of freedom. In particular, an anisotropic thermal conductivity, comparable in magnitude to that of metallic systems, was observed in quasi-one-dimensional (1D) spin- $\frac{1}{2}$ chain and ladder compounds with a large part of the heat current attributed to magnetic excitations.^{1,2,3,4,5,6,7} In the quasi-2D and some quasi-1D materials various other effects were observed including strong increase of the thermal conductivity by a modest magnetic field^{8,9,10,11} and enhanced scattering due to suppression of the gap in the spin-gapped materials.^{12,13} The thermal transport anomalies in layered cuprates associated with the magnetic and/or stripe excitations have also been found.^{14,15,16,17,18}

Both the strength and the temperature range for these new effects are very different from their counterparts in 3D magnetic materials, where the heat transport by well-defined magnetic excitations exist only well below the corresponding 3D ordering transition temperature.^{19,20,21} Note that the thermal transport in low-dimensional magnets has been studied before^{22,23,24} and the qualitative reasons for that difference has been understood. In 2D systems magnetic excitations can be

very well defined in a paramagnetic phase because of the large in-plane magnetic correlation length²⁵ and in 1D systems the soliton-like excitations can exist without any long-range order.²⁶

Theories. However, only recently a considerable progress in the theoretical understanding of the transport properties of 1D quantum spin systems has been made.^{27,28,29,30,31,32,33,34,35,36,37,38} The main focus of these recent studies has been on the relationship of the spin transport and conservation laws,^{27,28} specifically on the possibility of an ideal conducting state in one-dimensional integrable and non-integrable systems.^{31,32,33} While this problem is of significant interest, the importance of the spin-phonon and spin-impurity couplings, which break down the integrability of the underlying spin-only models, has also been discussed.^{36,37,38} In particular, it was obtained within the memory matrix formalism that the interplay of Umklapp scattering and spin-phonon coupling leads to the exponential temperature dependence of the thermal conductivity $\kappa \propto e^{T^*/T}$, with T^* proportional to the phonon’s Debye energy Θ_D .^{37,38}

Boltzmann equation approach. In the present work³⁹ we consider the problem of anomalous heat transport in quasi-1D spin-chain systems under a somewhat different perspective. First, we derive microscopically a model of 1D spin-boson excitations interacting with the 3D phonon environment and impurities, where the

spin-boson representation of the 1D Heisenberg model is obtained by performing the standard Jordan-Wigner transformation followed by bosonization.⁴⁰ It is assumed that the spin-boson velocity is large in comparison with the phonon velocity, $v \gg c$. The limit $v \gg c$ ($J \gg \Theta_D$) corresponds to the experimental situation in Sr_2CuO_3 , SrCuO_2 , $(\text{La,Ca,Sr})_{14}\text{Cu}_{24}\text{O}_{41}$, and other cuprate materials^{41,42} where $J \sim 2000\text{K}$ and $v/c \sim 10$. This large difference in spin and phonon energy scales is also responsible for the fact that, experimentally, the “spin peak” in thermal conductivity occurs at the temperatures well above the “phonon peak”.^{1,2,3,4,5,6,7} With this assumption and in the limit of weak spin-lattice coupling we solve the Boltzmann equation for the spin-boson distribution function and find the spin-phonon relaxation time τ_{sp} .

Normal vs Umklapp. Why τ_{sp} is important? Generally, the relaxation of the heat current and the resulting finite thermal conductivity should be due to the Umklapp processes or any other processes which do not conserve momentum. Since the characteristic “bandwidth” for the spin excitations in the real 1D spin chains materials of interest is very large ($J \sim 2000\text{K}$) in comparison with the experimental temperature range, the Umklapp scattering of spin excitations on themselves is strongly suppressed (as $\sim e^{-J/T}$). Instead, by considering the limit $v/c \gg 1$, we propose that the leading relaxation mechanism at not too low temperatures is the two-stage, bottle-neck process of (i) transferring momentum from the spin system to phonons, and (ii) subsequent dissipation of the phonon momentum via an Umklapp process or impurity scattering. The central idea is that the excess momentum of a spin-boson waits the longest time to get transferred to phonons, but once it is transferred it relaxes quickly. In other words, the phonon relaxation time τ_{pp} due to phonon-phonon scattering is much shorter than the spin-phonon relaxation time τ_{sp} , i.e. $\tau_{pp} \ll \tau_{sp}$. As a result, the relaxation rate of such a two-stage process is determined by the “normal” spin-phonon scattering rate $\tau_{2-st}^{-1} = [\tau_{sp} + \tau_{pp}]^{-1} \approx \tau_{sp}^{-1}$. The inequality $\tau_{pp} \ll \tau_{sp}$ can be justified qualitatively with the help of the following argumentation. First, the spin-lattice coupling is weak. Second, since $c \ll v$ the phonon states have a significant thermal population at the temperatures where the spin contribution to the transport is substantial.

Furthermore, there is also a kinematic argument in favor of $\tau_{pp} \ll \tau_{sp}$ that results from our analysis. The leading contribution to the transport comes from the spin bosons with a small momentum $k \ll T/v$. We find that the most effective scattering mechanism for such bosons is an absorption of a “thermal” phonon, that is a phonon whose energy is of the order of T and momentum is of the order $P_T = T/c \gg T/v \gg k$. For finite T such phonons have finite relaxation time τ_{pp}^T . We will show that the spin bosons in question have a divergent relaxation time $\tau_{sp}(k) \propto 1/k^2$. Therefore, for spin bosons with sufficiently small k ’s the relevant phonon relaxation time τ_{pp}^T is shorter than the spin-phonon relaxation time τ_{sp} not

only because of the weak spin-phonon coupling, but also due to the smallness of the characteristic momentum of the spin-boson, $P_T \gg k$.

We have performed a detailed study of the kinematics of the spin-phonon scattering processes and obtained the corresponding transport relaxation rate $\tau_{sp}^{-1} \simeq \mathcal{A}k^2T^3/v^3$ for $T \ll \Theta_D$, and $\tau_{sp}^{-1} \simeq \mathcal{A}k^2T\Theta_D^2/v^3$ for $T \gtrsim \Theta_D$, \mathcal{A} is a constant related to the spin-phonon coupling, $\mathcal{A} \propto (g_{sp}/c)^2$. The characteristic power of k^2 in the relaxation rate can be traced back to the fact that spin excitations are confined to lower dimensions than phonons. The latter implies that it is only the momentum along the chains which is conserved in the spin-phonon scattering. This, in turn, leads to a larger scattering space for phonons and makes relaxation rate of the spin bosons $\propto k^2$. Note that for the problem of the phonon-phonon scattering in 3D the phonon scattering rate is $\propto k^4$ because the scattering space is restricted by the momentum conservation in all three dimensions.⁴³ The temperature dependence of the relaxation rate is due to the bosonic nature of both the spin excitations and the phonons. Thus, the spin-phonon relaxation rate obtained in this work should apply to other low-dimensional spin systems as well.

Infrared divergence. However, one can find that the considered scattering mechanism becomes too weak at low energy and ineffective for the dissipation of the low-energy spin bosons. Namely, within the formalism of Boltzmann equation, $\tau_{sp}^{-1} \propto k^2$ leads to the infrared diverging thermal conductivity $\kappa_s \propto \int dk/k^2 \sim k^{-1}|_{k_0}$, $k_0 \rightarrow 0$, the situation familiar from the phonon thermal conductivity in 3D insulators.^{43,44,45,46} In that latter 3D phonon problem the regularization of such a divergence is non-trivial and involves a consideration of the higher-order phonon processes,^{44,47} degeneracy of phonon branches at high symmetry points,⁴⁸ or scattering on boundaries.

Impurities. What physical effect can render κ_s finite in our case? In contrast with the 3D systems,⁴⁹ because of the 1D nature of spins, even a weak impurity potential will have a dramatic effect on the low-energy spin bosons. The impurities generate a relevant interaction in the renormalization group (RG) sense. That is, they scatter low-energy excitations very well destroying their quasi-ballistic propagation. Below the so-called Kane-Fisher scale T_{KF} the scattering is very strong and leads to the localization of 1D excitations.⁵⁰ On the other hand, at the temperatures well above this scale $T \gg T_{KF}$ the impurity scattering can be analyzed perturbatively. As a consequence of such an analysis we find that impurities result in the momentum-independent scattering rate $\tau_{imp}^{-1} \propto nT^{-1}$, n being the impurity concentration. Total scattering rate $\tau_{tot}^{-1} = \tau_{sp}^{-1} + \tau_{imp}^{-1}$ is finite at $k = 0$, which makes κ_s finite.

Results. Altogether, the combined effect of impurities and the spin-phonon scattering leads to the following spin-boson thermal conductivity behavior: (i) in the low-temperature, impurity-scattering dominated regime

$\kappa_s \propto T^2$, (ii) in the spin-phonon scattering dominated regime, intermediate temperatures $T_m \ll T \ll \Theta_D$, $\kappa_s \propto T^{-1}$, and (iii) in the spin-phonon scattering dominated regime, higher temperatures $T \gtrsim \Theta_D$, $\kappa_s = \text{const} \propto T_m/\Theta_D$. Here the temperature T_m corresponds to the maximum in $\kappa_s(T)$. It is also the crossover temperature between the impurity- and phonon-scattering dominated regimes.

We find that this temperature behavior of the thermal conductivity agrees very well with the available experimental data for the spin-chain material Sr_2CuO_3 .^{5,6} The thermal conductivity for the zig-zag chain SrCuO_2 and the spin-ladder compounds $(\text{Ca}, \text{La}, \text{Sr})_{14}\text{Cu}_{24}\text{O}_{41}$,^{1,5} whose underlying spin models are different from the ones considered in this work, is briefly discussed.

We analyze the impurity concentration dependence of several quantities. As a result we predict an unusual behavior of: (i) the crossover temperature $T_m \propto n^{1/6}$, (ii) the spin-boson thermal conductivity maximum value $\kappa_s^{\text{max}} = \kappa_s(T_m) \propto n^{-2/3}$, and (iii) the asymptotic value of κ_s at $T \gg T_m$: $\kappa_s^\infty \propto n^{-1/2}$.

Outline. Our paper is organized as follows. In Sec. II we introduce the spin-chain Hamiltonian and derive the spin-phonon and spin-impurity interaction terms. In Sec. III we find the spin-boson relaxation time due to scattering off the phonons. In Sec. IV the impurity contribution to the spin-boson relaxation time is calculated. In Sec. V the thermal conductivity *vs* temperature is obtained and the results are compared to experimental data. In Section V we also put forward several theoretical predictions for the impurity concentration dependence of different quantities and suggest further experiments. In Sec. VI we discuss the notion of the mean free path and its applicability to the transport by the long-wavelength spin bosons. We conclude by Sec. VII which contains the discussion of our approach and approximations. Technically involved details concerning the spin-phonon collision integral and impurity scattering are described in Appendix A and Appendix B, respectively.

II. SPIN-PHONON AND SPIN-IMPURITY INTERACTION HAMILTONIANS

Spin-chain Hamiltonian. The Hamiltonian of a single Heisenberg antiferromagnetic spin- $\frac{1}{2}$ chain is:

$$H_{\text{chain}} = J \sum_i \mathbf{S}_i \cdot \mathbf{S}_{i+1}. \quad (1)$$

This Hamiltonian, after the Jordan-Wigner transformation, can be expressed in terms of fermionic operators ψ_i as follows:

$$H_{JW} = -\frac{J}{2} \sum_i \left(\psi_i^\dagger \psi_{i+1} + \text{h.c.} + \frac{1}{2} \left(2\psi_i^\dagger \psi_i - 1 \right) \left(2\psi_{i+1}^\dagger \psi_{i+1} - 1 \right) \right). \quad (2)$$

It is convenient to bosonize this Hamiltonian. To do that one introduces chiral fermionic fields $\psi_{L,R}(x)$ such that $\psi(x) \approx \psi_L(x)e^{ik_F x} + \psi_R(x)e^{-ik_F x}$. These fields can be rewritten in terms of spin boson field $\Phi(x)$ and its dual field $\Theta(x)$ as

$$\psi_{L,R} = \frac{1}{\sqrt{\pi a}} e^{i\sqrt{\pi}(\Theta \pm \Phi)}. \quad (3)$$

Using Φ, Θ one writes the spin-chain Hamiltonian as:

$$H_0 = \frac{v}{2} \int dx \left(\mathcal{K} (\partial_x \Theta)^2 + \mathcal{K}^{-1} (\partial_x \Phi)^2 \right), \quad (4)$$

where $\int dx \equiv \int_{-L/2}^{L/2} dx$, L is the linear size of the system, the Luttinger-liquid parameter \mathcal{K} is equal to $1/2$, and the spin-boson velocity v is given by

$$v = \frac{\pi}{2} J a, \quad (5)$$

where a is the chain lattice constant. Furthermore, the spin-boson variables are redefined according to the rules:

$$\begin{aligned} \tilde{\Theta} &= \mathcal{K}^{1/2} \Theta, \\ \tilde{\Phi} &= \mathcal{K}^{-1/2} \Phi. \end{aligned} \quad (6)$$

Then we introduce the creation and annihilation operators for the field $\tilde{\Phi}(x)$:

$$\tilde{\Phi}(x) = \sum_k \frac{e^{ikx}}{\sqrt{2L|k|}} \left(b_k^\dagger + b_{-k} \right), \quad (7)$$

which diagonalize the Hamiltonian H_0 , Eq. (4):

$$H_0 = v \sum_k |k| b_k^\dagger b_k. \quad (8)$$

For details of this procedure see Ref. 40. We would like to note that the Hamiltonian for the spin- $\frac{1}{2}$ chain contains other terms beyond the LL form above. These terms do not lead to the finite heat conductivity by themselves and thus are not included in our consideration. The role of such terms in the presence of phonons via a phonon-phonon-assisted Umklapp process has been considered elsewhere.³⁷

Spin-Phonon Hamiltonian. Since the superexchange J is a function of inter-site separation, the lattice vibrations are able to modify it. This mechanism will, therefore, couple phonons to the spin degrees of freedom. We can account for this coupling by expanding J in gradients of inter-site distance $a\partial_x u_x$:

$$J(a + a\partial_x u_x) = J(a) + \delta J \partial_x u_x + \dots \quad (9)$$

where u_x is the displacement along the chain. This translates into the following interaction Hamiltonian:

$$H_{\text{int}} = \frac{g_{sp}}{2} \int dx \left(\mathcal{K} (\partial_x \Theta)^2 + \mathcal{K}^{-1} (\partial_x \Phi)^2 \right) (\partial_x u_x), \quad (10)$$

where $g_{sp} = \delta J a$ is a spin-phonon coupling constant. The atomic displacement vector \mathbf{u} can be expressed in terms of phonon creation and annihilation operators as follows:

$$\mathbf{u}(\mathbf{R}) = \frac{1}{\sqrt{N}} \sum_{\mathbf{P}\ell} \frac{e^{i\mathbf{P}\mathbf{R}}}{\sqrt{2m_i\omega_{\mathbf{P}\ell}}} \boldsymbol{\xi}_{\mathbf{P}\ell} \left(a_{\mathbf{P}\ell}^\dagger + a_{-\mathbf{P}\ell} \right), \quad (11)$$

where $\omega_{\mathbf{P}\ell} = c_\ell |\mathbf{P}|$ and summation runs over the three-dimensional wave-vector \mathbf{P} and over three polarizations of 3D phonons denoted by ℓ . Here $\boldsymbol{\xi}$ is the polarization vector of a phonon, m_i is the mass of the unit cell, N is the number of unit cells in the sample, $\mathbf{R} = (x, y, z)$ is the position vector. Sound velocities c_ℓ are much smaller than the spin-boson velocity v :

$$c_\ell \ll v. \quad (12)$$

For a chain specified by $y = 0, z = 0$ the interaction Hamiltonian, Eq. (10), can be written, using Eqs. (11) and (7), as:

$$H_{sp} = -\frac{ig_{sp}}{\sqrt{N}} \sum_{kk'\mathbf{P}\ell} V_\ell(\mathbf{P}, k, k') \left(a_{\mathbf{P}\ell}^\dagger b_k^\dagger b_{k'} + \text{h.c.} \right), \quad (13)$$

with

$$V_\ell(\mathbf{P}, k, k') = \frac{P_\parallel k k'}{\sqrt{8m_i\omega_{\mathbf{P}\ell} k k'}} (\boldsymbol{\xi}_{\mathbf{P}\ell})_x \delta_{P_\parallel, k' - k}, \quad (14)$$

where k and k' are the 1D momenta of spin bosons and \mathbf{P} is the 3D momentum of a phonon. Note that only component of the total momentum along the chain is conserved, which is explicitly given by the δ -symbol. The projection of the polarization vector on the x -axis $(\boldsymbol{\xi}_{\mathbf{P}\ell})_x$ is equal to:

$$(\boldsymbol{\xi}_{\mathbf{P}\ell})_x = \begin{cases} |P_\parallel|/|\mathbf{P}| & \text{longitudinal,} \\ \sqrt{1 - (P_\parallel/|\mathbf{P}|)^2} & \text{transverse,} \\ 0 & \text{transverse,} \end{cases} \quad (15)$$

where two answers for the transverse phonons correspond to two possible choices of polarization $\boldsymbol{\xi}$. It is convenient to choose the first of these polarizations to lie in the plane given by \hat{x} and \mathbf{P} and the second one to be normal to this plane. Since the projection $\boldsymbol{\xi}_x$ is zero in the second case, such phonons do not couple to the spin bosons and are not discussed in this paper any further.

Altogether, the Hamiltonian (13) describes emission and absorption of phonons by the spin-density excitations represented by the spin bosons, see Fig. 1.

Spin-Impurity Hamiltonian. In addition to interacting with phonons spin bosons are also scattered on impurities. Microscopically, the origin of that effect is simple: impurity leads to a local variation of the superexchange coupling J , which leads to scattering of magnetic excitations. The impurities affect the low temperature transport properties of the Tomonaga-Luttinger liquid in a dramatic way because they act as almost ideal backward

scatterers for the low-lying excitations. The most important (relevant in RG sense) part of the impurity Hamiltonian for an impurity located at x_0 can be written as:

$$\begin{aligned} H_{\text{imp}} &= a\delta J_{\text{imp}} e^{-ik_F x_0} \psi_L^\dagger(x_0) \psi_R(x_0) + \text{h.c.} \\ &= \frac{\delta J_{\text{imp}}}{\pi} \cos\left(2k_F x_0 + \sqrt{2\pi}\Phi(x_0)\right). \end{aligned} \quad (16)$$

Although the effect of impurities is very strong for the low-lying excitations, for small $\delta J_{\text{imp}} \ll J$ and not too low temperatures the impurity scattering can be considered perturbatively.

III. PHONON MECHANISM OF RELAXATION

Boltzmann equation. In order to study the relaxation of spin excitations on phonons we will solve the Boltzmann equation for spin bosons coupled to the bath of 3D phonons. The stationary Boltzmann equation has the form:

$$v\partial_x f_k = -S_k[f], \quad (17)$$

where f_k is the spin-boson distribution function and $S_k[f]$ is the collision integral. In general, the collision integral is a non-linear functional of both f_k and the phonon distribution function $n_{\mathbf{P}\ell}$: $S_k = S_k[f, n]$. However, as we argued in the Introduction, one can assume that the relaxation of phonons is quicker than that of the spin bosons. Thus, even in the presence of the temperature gradient $\partial_x T$, phonons will be treated as if they are in a local equilibrium with themselves and this equilibrium is characterized by a local temperature $T(x) = T_0 + x\partial_x T$:

$$n_{\mathbf{P}\ell} = n_{\mathbf{P}\ell}^0(T(x)) = \frac{1}{e^{\omega_{\mathbf{P}\ell}/T(x)} - 1}. \quad (18)$$

Therefore, one can write $S_k \approx S_k[f, n^0] = S_k[f]$.

Collision integral. The collision integral for spin bosons can be generally written as:

$$S_k = \int_{k'} \left[W_{kk'} f_k (f_{k'} + 1) - W_{k'k} f_{k'} (f_k + 1) \right], \quad (19)$$

where $\int_{k'}$ stands for $\int dk'/2\pi$ and $W_{kk'}$ is the total probability of the spin excitation to be scattered from the state k to the state k' . For the processes of scattering due to phonons such probabilities are given by:

$$W_{kk'} = \sum_{\ell} \int_{\mathbf{P}} \left(w_{kk'\mathbf{P}}^\ell (n_{\mathbf{P}\ell}^0 + 1) + w_{k'k\mathbf{P}}^\ell n_{\mathbf{P}\ell}^0 \right), \quad (20)$$

where the symbol $\int_{\mathbf{P}}$ stands for $(1/2\pi)^3 \int d^3\mathbf{P}$. Similar expression for the probability $W_{k'k}$ of scattering from k' to k can be obtained by permutation of k and k' in (20). Here the “elementary” scattering probabilities $w_{kk'\mathbf{P}}^\ell$ of the spin boson due to emission or absorption of

the phonon with the momentum \mathbf{P} and polarization ℓ are determined from Eqs. (13), (14):

$$w_{kk'\mathbf{P}}^\ell = \frac{g_{sp}^2 V_0}{8m_i} \cdot \frac{P_\parallel^2 |kk'|}{\omega_{\mathbf{P}\ell}} (\xi_\ell)_x^2 \times \delta(k' + P_\parallel - k) \delta(\omega_{k'} + \omega_{\mathbf{P}\ell} - \omega_k), \quad (21)$$

where V_0 is elementary cells volume, $\omega_k = v|k|$ is the spin-boson energy. In all the collisions the total energy and the projection of the momentum along the chain is preserved. These conservation laws are enforced by the δ -functions in Eq. (21).

Linearized Boltzmann equation. Boltzmann equation (17) should be solved in the presence of a non-zero temperature gradient $\partial_x T \neq 0$. Assuming that the gradient $\partial_x T$ is small one can introduce a usual ansatz for the distribution function f_k to linearize the Boltzmann equation:

$$f_k = f_k^0 + f_k^1, \quad (22)$$

$$f_k^0(T) = \frac{1}{e^{\omega_k/T} - 1},$$

where f_k^1 is a non-equilibrium correction to the equilibrium distribution function f_k^0 . Function f_k^1 is considered to be small. Since the collision integral vanishes identically in an equilibrium state when $f_k = f_k^0$ and $n_{\mathbf{P}} = n_{\mathbf{P}}^0$, one expects that f_k^1 should be proportional to the temperature gradient $\partial_x T$.

Thus, the Boltzmann equation for the spin bosons to the first order in $\partial_x T$ can be rewritten as:

$$\frac{v|k|}{T} (\partial_x T) \frac{\partial f_k^0}{\partial k} = S_k, \quad (23)$$

where S_k now stands for the linearized collision integral which can be expressed using the notations of Eq. (22) as:

$$S_k = \sum_\ell \left(S_{k\ell}^{(1)} + S_{k\ell}^{(2)} \right), \quad (24)$$

$$S_{k\ell}^{(1)} = \int_{k'\mathbf{P}} w_{kk'\mathbf{P}}^\ell \left[(n_{\mathbf{P}\ell}^0 + f_{k'}^0 + 1) f_k^1 + (f_k^0 - n_{\mathbf{P}\ell}^0) f_{k'}^1 \right], \quad (25)$$

$$S_{k\ell}^{(2)} = - \int_{k'\mathbf{P}} w_{k'\mathbf{P}}^\ell \left[(n_{\mathbf{P}\ell}^0 + f_k^0 + 1) f_{k'}^1 + (f_{k'}^0 - n_{\mathbf{P}\ell}^0) f_k^1 \right]. \quad (26)$$

The integral $S^{(1)}$ accounts for two types of collision events: (i) spin boson with the momentum k emits a phonon with the momentum \mathbf{P} and scatters into the state with the momentum k' ; (ii) process inverse to (i). Likewise, $S^{(2)}$ describes the absorption of a phonon by spin boson with the momentum k and the corresponding inverse process, see Fig. 1.

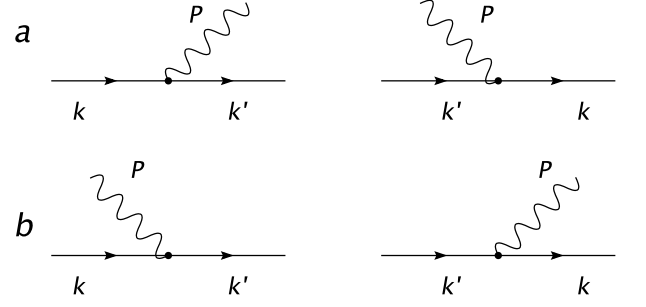


FIG. 1: The scattering diagrams of the spin boson on the phonon for the processes contributing to the collision integral (a) $S^{(1)}$ and (b) $S^{(2)}$. Solid lines are spin bosons, wavy lines are phonons.⁵¹

Once the Boltzmann equation (23) is solved for f_k^1 the spin-boson thermal current density J_E^s can be written as:

$$J_E^s = \int v^2 k f_k^1 \frac{dk}{2\pi} = -\kappa_s \partial_x T, \quad (27)$$

where the coefficient κ_s is the spin-boson thermal conductivity. The total thermal conductivity observed in experiment is the sum of κ_s and the phonon thermal conductivity.

Kinematic considerations. To solve the Boltzmann equation (23) one needs to evaluate integrals in Eqs. (25) and (26). Part of this task can be accomplished without any approximations as the integral over \mathbf{P} in $S^{(1)}$ and $S^{(2)}$ can be calculated explicitly. Because of the conservation laws discussed above the remaining integration over k' will be restricted to some finite intervals whose extent and range depend on k . Mathematical details of these calculations are given in Appendix A.

The collision integral derivation can be simplified even more if we restrict our attention to the spin bosons whose energies are small: $v|k| \ll \min\{T; \Theta_D\}$. These energies are the most important since the transport is dominated by the bosons with small k . Such an approximation is used at various stages of S_k calculation. The consistency of our result with this latter assumption can be verified afterward.

Relaxation time. One can write the collision integral in Eq. (24) as a sum of two terms:

$$S_k = \frac{f_k^1}{\tau_{sp}(k)} + \delta S_k, \quad (28)$$

where the first term has the usual relaxation time form, while the second one does not. However, the second term can be estimated and it is shown to be small for small spin-boson energy $\delta S_k / S_k \propto (vk/T)^2$ (for details see Appendix A).

Finally, with the help of these approximations, the collision integral can be written in the relaxation time form $S_k \approx f_k^1 / \tau_{sp}(k)$, where $\tau_{sp}(k)$ is the transport relaxation time. Since the transport is dominated by the spin

bosons with small momentum, one can use that smallness to simplify significantly the corresponding expression (A14) in the collision integral to obtain:

$$\frac{1}{\tau_{\text{sp}}(k)} = \frac{\tilde{\mathcal{A}}vk^2}{T} \int_0^{\Theta_D/v} \frac{dk'}{2\pi} \frac{(k')^3}{2\sinh^2(vk'/2T)}, \quad (29)$$

where $\tilde{\mathcal{A}}$ is a constant proportional to the spin-lattice coupling, $\sinh(\dots)$ comes from the bosonic distribution function, and powers of k and k' are from the scattering amplitudes $V(\mathbf{P}, k, k')$ in Eq. (14) and due to the integration over \mathbf{P} .

What does this formula tell us about the most effective scattering process for a spin boson with small momentum? One can see that the major contribution to the integral in (29) comes from $vk' \sim \min\{T; \Theta_D\}$. That is, the scattered spin boson is “thermalized”. Therefore, the most important scattering process is the absorption of a thermalized phonon.

Further simplification of the problem can be achieved by exploiting the small parameter $c/v \ll 1$. Because the spin bosons are fast, the energy and momentum conservation dictates that the majority of the phonons which interact with the spin subsystem must have their momentum almost normal to the chain direction. Indeed, the energy conservation gives that the phonon momentum $P = \omega_{\mathbf{P}}/c = (v/c)[|k| - |k'|]$, where k and k' are the 1D spin-boson momenta, while the momentum conservation along the chain gives $|P_{\parallel}| = |k - k'|$. Therefore, the momentum component perpendicular to the chain for a typical phonon is: $|P_{\perp}| \approx P \sim (v/c)|P_{\parallel}| \gg |P_{\parallel}|$, except for the case of almost elastic backward scattering $k' \approx -k$. The latter scattering event does not contribute substantially to the transport relaxation time (see Appendix A). Since the momentum \mathbf{P} is almost normal to the chain the corresponding projection of the polarization vector for the longitudinal phonons given in Eq. (15) is small: $\xi_{xl} = \mathcal{O}(c/v)$. At the same time the transverse phonon polarization projection is $\xi_{xt} = \mathcal{O}(1)$. Thus, the most effective spin-phonon scattering is due to the transverse phonons.

We would like to rewrite Eq. (29) in the following form:

$$\frac{1}{\tau_{\text{sp}}(k)} = \frac{\mathcal{A}k^2T^3}{v^3} \Gamma(\Theta_D/T), \quad (30)$$

with the auxiliary function $\Gamma(z)$ defined as:

$$\Gamma(z) = \frac{I_1(z)}{I_1(\infty)}, \quad I_1(z) = \int_0^z \frac{x^3 dx}{2\sinh^2 x/2}, \quad (31)$$

and \mathcal{A} given by:

$$\mathcal{A} = \frac{I_1(\infty)}{2\pi} \tilde{\mathcal{A}} \propto \frac{V_0}{m_i} \left(\frac{g_{sp}}{c} \right)^2. \quad (32)$$

$I_1(\infty) = 12\zeta(3)$ where $\zeta(x)$ is the zeta-function. One can easily verify that:

$$\Gamma(\Theta_D/T) = \begin{cases} 1 & \text{for } T \ll \tilde{\Theta}_D, \\ (\tilde{\Theta}_D/T)^2 & \text{for } T \gg \tilde{\Theta}_D, \end{cases} \quad (33)$$

where $\tilde{\Theta}_D = \Theta_D/\sqrt{I_1(\infty)} \approx \Theta_D/4$ plays the role of a crossover temperature. That is, for the temperatures well below the Debye energy $T \ll \Theta_D$ the integration in Eq. (30) is restricted by $\sinh^{-2}(x/2)$ and the relaxation rate is given by:

$$\frac{1}{\tau_{\text{sp}}(k)} = \frac{\mathcal{A}T^3k^2}{v^3}. \quad (34)$$

However, for the temperatures comparable to Θ_D and higher (in fact, for $T \gtrsim \Theta_D/4$) the integration limit in Eq. (31) becomes small. This leads to the change in the temperature dependence of the relaxation rate from $\propto T^3$ to $\propto T$:

$$\frac{1}{\tau_{\text{sp}}(k)} = \frac{\mathcal{A}\tilde{\Theta}_D^2Tk^2}{v^3}. \quad (35)$$

The relaxation rate for the spin boson due to scattering on phonons in the form given in Eq. (30) with the limiting cases given by Eqs. (34) and (35) are the main results of this Section.

It is instructive to inspect and compare our results with the well-known phonon-phonon scattering rate for the 3D phonons, studied in detail many years ago.^{43,45,48} For the 3D phonon-phonon scattering rate one finds that it depends on the higher power of the wave-vector $\propto k^4$, while its temperature dependence is the same. This is because the scattering space in phonon-phonon case is restricted by the momentum conservation in all three dimensions. In our case, it is only the momentum along the chains which is conserved in the spin-phonon scattering. This leads to fewer restrictions and a larger scattering space for phonons and makes the relaxation rate $\propto k^2$. Thus, the characteristic power of k^2 in the relaxation rate Eqs. (29)-(35) can be traced back to the fact that spin excitations are confined to lower dimensions than phonons. This implies that our results for the spin-phonon relaxation rate should be applicable to other low-dimensional spin systems as well. The temperature dependence of the relaxation rate is due to the bosonic nature of both the spin excitations and the phonons.

Infrared divergence. With the collision integral in the relaxation time form the Boltzmann equation is trivially solved:

$$f_k^1 = \frac{v|k|\tau_{\text{sp}}(k)}{T} (\partial_x T) \frac{\partial f_k^0}{\partial k} \approx -\frac{\tau_{\text{sp}}(k)}{k} (\partial_x T), \quad (36)$$

where we used that $(v|k|/T)\partial f^0/\partial k \approx -1/k$ in the small k limit.

Once f_k^1 is found the energy current density can be determined from Eq. (27) which yields the thermal conductivity:

$$\kappa_s = \int v^2 \tau_{\text{sp}}(k) \frac{dk}{2\pi} = \frac{v^5}{2\pi \mathcal{A} T^3} \int_0^{T/v} \frac{dk}{k^2}. \quad (37)$$

This expression diverges at small k giving rise to an infinite κ_s . The divergence happens because the scattering of spin bosons on phonons is not sufficiently

strong for $k \rightarrow 0$ to ensure the convergence of the low-energy contribution to the thermal conductivity. Such a situation is familiar from the phonon thermal conductivity in 3D insulators.^{43,44,45,46} In the 3D phonon problem the regularization of such a divergence is non-trivial and involves consideration of the higher-order phonon scattering processes,^{44,47} degeneracy of different phonon branches at high symmetry points,⁴⁸ and interface boundary scattering.

We would like to note here that such a divergence is not related to any conservation law or integrability of the problem. The scattering simply becomes too weak at low energies and is unable to equilibrate the excitations. A model example of such a behavior would be a system of free, noninteracting phonons in a continuum, which are scattered only by the point-like impurities according to the Rayleigh's law.⁴⁹ All the conservation laws are broken in this case. Yet, the heat conductivity is infinite in such a system since the Rayleigh scattering is ineffective at low energies, which leads to a diverging integral similar to our Eq. (37).

In our case, because of the 1D nature of spin system the impurity scattering of spin bosons is very effective at low energies, as we will show in the next Section, so that even weak impurity potential renders the thermal conductivity finite.

IV. IMPURITY SCATTERING

In a 1D system impurities have a dramatic effect on the low-energy excitations. The Hamiltonian for spin excitations in a 1D spin chain interacting with a single defect is given in Eq. (16). Since the impurity Hamiltonian is a relevant perturbation in the RG sense, defects scatter the low-energy excitations very effectively destroying their quasi-ballistic propagation. Therefore, the disorder in the magnetic coupling J will remove the infrared divergence in Eq. (37).

The impurity Hamiltonian in Eq. (16) is not a low-order polynomial of the bosonic field. Thus, it is impossible to account for the impurity scattering within the formalism of the Boltzmann transport theory. Instead, we will evaluate the spin boson life-time τ_{imp} using the Green's function perturbative expansion in powers of δJ_{imp} .

There are two issues we must clarify before proceeding with this approach. First, below the Kane-Fisher temperature the impurity scattering is very strong and leads to the localization of 1D excitations.⁵⁰ On the other hand, at the temperatures well above this scale the impurity contribution can be analyzed perturbatively. Thus, for the perturbation theory in powers of δJ_{imp} to be valid the temperature must be bigger than the Kane-Fisher temperature⁵⁰:

$$T \gg T_{\text{KF}} = J \left(\frac{\delta J_{\text{imp}}}{J} \right)^{\frac{1}{1-\kappa}} = \frac{\delta J_{\text{imp}}^2}{J}. \quad (38)$$

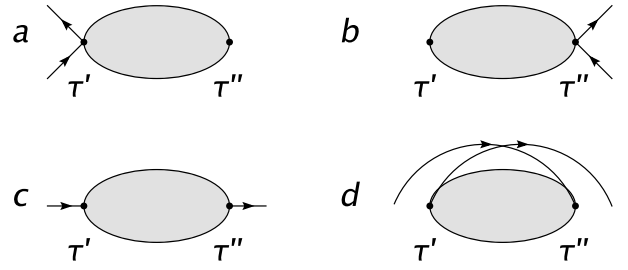


FIG. 2: Second-order diagrams for the spin-boson scattering on impurities. Vertices represent interactions with impurities at times τ' and τ'' . Shaded ellipses emphasize that there is a summation over virtual states with any number of spin-boson excitations. This is due to the fact that the interaction Hamiltonian is exponential in the bosonic field. Formally, the ellipses correspond to $\langle e^{i\sqrt{2\pi}\tilde{\Phi}(0,\tau')} e^{i\sqrt{2\pi}\tilde{\Phi}(0,\tau'')} \rangle$.⁵¹

Second, it is important to note that, generally, the life-time of an excitation is not equivalent to the transport relaxation time. While the only processes which violate the conservation of the momentum contribute to the latter, any kind of scattering shortens the former. However, since Eq. (16) does not conserve momentum and since in any typical scattering event the spin-boson momentum changes drastically, there is no distinction between these two time scales in our case. This justifies the use of our approach.

The correction to the single-boson Green's function from the impurity scattering is evaluated as follows. The lowest-order single impurity contribution to the Green's function is:

$$\mathcal{D}_k(\tau) - \mathcal{D}_{0k}(\tau) \approx \int \left\langle \left(b_k^\dagger(\tau) + b_{-k}(\tau) \right) \times \right. \quad (39) \\ \left. H_{\text{imp}}(\tau') H_{\text{imp}}(\tau'') \left(b_{k'}(0) + b_{-k'}^\dagger(0) \right) \right\rangle_{\text{connected}} d\tau' d\tau''.$$

The right hand side of this equation is proportional to the self-energy. Since the impurity breaks the translational invariance the self-energy depends on two momenta. As usual, the translational invariance will be restored after averaging over the random impurity positions. Since the perturbation H_{imp} , Eq. (16), is an exponential in the bosonic field $\tilde{\Phi}$ rather than a polynomial, the calculation of the Matsubara average involves an effective summation of an infinite number of terms, as schematically shown in Fig. 2. Details of such a procedure are given in Appendix B. As a result of our calculation the retarded self-energy is obtained through the analytical continuation of the Matsubara self-energy:

$$\Sigma_{k,\omega}^R \approx -i \frac{n \delta J_{\text{imp}}^2 \omega}{2aJ|k|T}, \quad (40)$$

with n being the dimensionless impurity concentration. Note that this self-energy is pure imaginary.

Once the self-energy is found one can obtain the

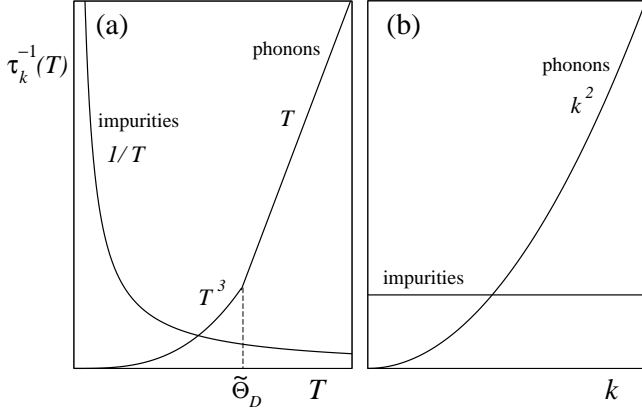


FIG. 3: The sketch of the spin-phonon and spin-impurity relaxation rates τ_{sp}^{-1} and τ_{imp}^{-1} as a function of (a) temperature, (b) momentum. In (a) $\tilde{\Theta}_D = \Theta_D/4$.

dressed Green's function:

$$D_{k,\omega} = \frac{D_{0k,\omega}}{1 - D_{0k,\omega} \Sigma_{k,\omega}^R}, \quad (41)$$

where

$$D_{0k,\omega} = \frac{2\omega_k}{\omega_k^2 - \omega^2}, \quad (42)$$

From here it is possible to find the lifetime of the spin bosons by solving equations on the poles of the Green's function: $1 = D_{0k,\omega} \Sigma_{k,\omega}^R$. This yields the following expression for τ_{imp}^{-1} :

$$\frac{1}{\tau_{imp}} = \frac{\Delta^2}{T}, \quad (43)$$

where

$$\Delta^2 \propto n \delta J_{imp}^2. \quad (44)$$

The details of the derivation are given in Appendix B. We would like to note that the impurity-induced relaxation rate $\tau_{imp}^{-1} \propto T^{-1}$ has been first obtained by Oshikawa and Affleck, Ref. 52, in the context of the theory of electron spin resonance in the S=1/2 quantum antiferromagnetic chains.

Unlike the spin-phonon scattering, the relaxation rate due to the disorder is independent of k . The impurity scattering provides an effective relaxation mechanism at low energies and thus removes the divergence of the thermal conductivity in Eq. (37) by effectively cutting off the low-energy spin bosons.

Our Fig. 3 gives a qualitative comparison of the temperature and k dependencies of the spin-phonon and spin-impurity relaxation rates τ_{sp}^{-1} and τ_{imp}^{-1} .

V. THERMAL CONDUCTIVITY

Cumulative result. Finally, having at hands the transport relaxation rates of the spin-boson due to scattering

on the phonons, Eq. (30), and on impurities, Eq. (43), we are adequately equipped to calculate the thermal conductivity of the spin chains. The total relaxation time is given by:

$$\frac{1}{\tau_{tot}(k)} = \frac{1}{\tau_{imp}} + \frac{1}{\tau_{sp}(k)}. \quad (45)$$

Then the solution of the Boltzmann equation which we had for the phonon scattering (36) should be modified to:

$$f_k^1 = \frac{v|k|\tau_{tot}(k)}{T} \frac{\partial f_k^0}{\partial k} (\partial_x T). \quad (46)$$

As a result the thermal current is given by:

$$J_E^s = \int_k v^2 k f_k^1 = (\partial_x T) \frac{v^3}{T} \int_k \frac{k|k|}{\tau_{imp}^{-1} + \tau_{sp}^{-1}} \frac{\partial f_k^0}{\partial k}. \quad (47)$$

Thus, using the explicit expressions for the spin-phonon and spin-impurity relaxation rates the following formula for the thermal conductivity can be obtained:

$$\kappa_s(T) = \frac{vT^2}{\pi\Delta^2} \int_0^{J/T} \frac{x^2 dx}{4 \sinh^2(x/2)} \frac{\alpha(T)}{x^2 + \alpha(T)}, \quad (48)$$

where $x = vk/T$ and

$$\alpha(T) = \frac{v^5 \Delta^2}{AT^6 \Gamma(\frac{\Theta_D}{T})} \quad (49)$$

with $\Gamma(z)$ defined in Eq. (31). Since the temperature is always much smaller than J one can safely replace the upper limit in Eq. (48) by infinity.

Our Eq. (48) specifies a function with the following properties. Depending on the value of Θ_D it either has a single maximum at some $T = T_m$ (larger $\tilde{\Theta}_D$) or is a monotonic function (smaller $\tilde{\Theta}_D$). In both cases this function vanishes as T^2 at $T \ll T_m$ and saturates at $T \gg T_m$. These qualitative features of $\kappa_s(T)$ can be easily established. Without impurities ($\Delta = 0$) the integral in Eq. (48) diverges at the lower limit. The impurity scattering cuts off this divergence. When the temperature is small the impurity scattering is much stronger than the typical spin-phonon scattering, which corresponds to $\alpha(T) \gg 1$. Thus, $\kappa_s \propto T^2$ at low temperatures. In the limit of larger temperatures the impurity scattering is much weaker than the spin-phonon one and $\alpha(T) \ll 1$. If we assume that the temperature is still much less than the Debye energy $T_m < T \ll \Theta_D$ then $\Gamma(\Theta_D/T) = 1$. Therefore, in this temperature range Eq. (48) yields $\kappa_s \propto T^2 \sqrt{\alpha(T)} \propto 1/T$. At yet higher temperatures $T \gtrsim \tilde{\Theta}_D$ the temperature behavior of the spin-phonon relaxation rate changes from $\propto T^3$ to $\propto T$, which is reflected in the change of $\Gamma(\Theta_D/T)$ from 1 to $\approx (\tilde{\Theta}_D/T)^2$, see Eqs. (30)-(35). This gives $\kappa_s \propto T^2 \sqrt{\alpha(T)} \propto T^0$. Altogether, assuming $\tilde{\Theta}_D$ is not

too small:

$$\kappa_s(T) \propto \begin{cases} T^2 & \text{for } T \ll T_m, \\ T^{-1} & \text{for } T_m \ll T \ll \tilde{\Theta}_D, \\ T^0 & \text{for } T \gg \tilde{\Theta}_D. \end{cases} \quad (50)$$

where $\tilde{\Theta}_D \approx \Theta_D/4$, as introduced in Sec. III. Note that the low-temperature, impurity-controlled thermal conductivity in the generic Luttinger liquids has been studied in Ref. 53 using the memory-matrix formalism. Our $\propto T^2$ result matches the result of that work for the Luttinger liquid parameter of the spin- $\frac{1}{2}$ chain $\mathcal{K} = 1/2$. As one can see from Eq. (50) our results do not support suggestion of $\kappa_s \propto \exp(T^*/T)$ made in the experimental work, Ref. 5. Below we will discuss the origin of the maximum and of the saturation value of κ_s , but first we compare with the available experimental data.

Comparison with experiments. To compare our results with experimental data it is convenient to rewrite the above expression for $\kappa_s(T)$, Eq. (48), using the “reduced” temperature units $t = T/T_m$ with T_m which corresponds to the maximum in the thermal conductivity:

$$\frac{\kappa_s(t)}{\kappa_s^{max}} = \frac{\gamma_1}{t^4 \Gamma(t)} \int_0^\infty \frac{x^2 dx}{4 \sinh^2(x/2)} \frac{1}{x^2 + \gamma_2/t^6 \Gamma(t)}, \quad (51)$$

where $\Gamma(t) \equiv \Gamma(\frac{\Theta_D}{T})$ from Eq. (31), and the constants γ_1 and γ_2 are chosen in such a way that the temperature $T = T_m$ indeed corresponds to a maximum in κ_s and that $\kappa_s(T_m)$ is indeed equal to κ_s^{max} . For $\tilde{\Theta}_D$ not too close to T_m the constants are: $\gamma_1 = 1.26$ and $\gamma_2 = 1.83$. Such a choice of variables simply replaces a combination of impurity- and lattice-related coupling constants encoded in our Δ and \mathcal{A} , whose actual values are generally unknown, by phenomenological constants T_m and κ_s^{max} , found from experiment. In fact, in the limit $\Theta_D \rightarrow \infty$ this procedure completely determines our $\kappa_s(t)$ given in Eq. (51) since there are no adjustable parameters left. The resulting $\kappa_s(T)$ for this limiting case is shown in Fig. 4 by the dashed line.

Once we changed the variables to Eq. (51) there is only one parameter to adjust: Θ_D . If we choose $\Theta_D = 11.6T_m$ we fit experimental data for the spin-chain compound Sr_2CuO_3 perfectly. For this material $T_m = 79.4\text{K}$ and $\kappa_s^{max} = 36.7\text{Wm}^{-1}\text{K}^{-1}$. Figure 4 shows the comparison of our results and experimental data, where the latter are shown by diamonds and the former is the solid line. Shaded area highlights the region where, experimentally, the phonon background subtraction creates a large uncertainty in the data.⁵

Note that at high temperatures $T \gg \tilde{\Theta}_D$ Eq. (51) yields the asymptotic value of the spin-boson thermal conductivity κ_s^∞ :

$$\frac{\kappa_s^\infty}{\kappa_s^{max}} = \frac{\pi\gamma_1}{2\sqrt{\gamma_2}} \frac{T_m}{\tilde{\Theta}_D} \approx 5.55 \frac{T_m}{\tilde{\Theta}_D}. \quad (52)$$

Therefore, when we fix Θ_D we fix κ_s^∞ as well. Our choice of Θ_D corresponds to $\kappa_s^\infty = 0.48\kappa_s^{max}$. In Fig. 4 κ_m^∞ is marked by an arrow.

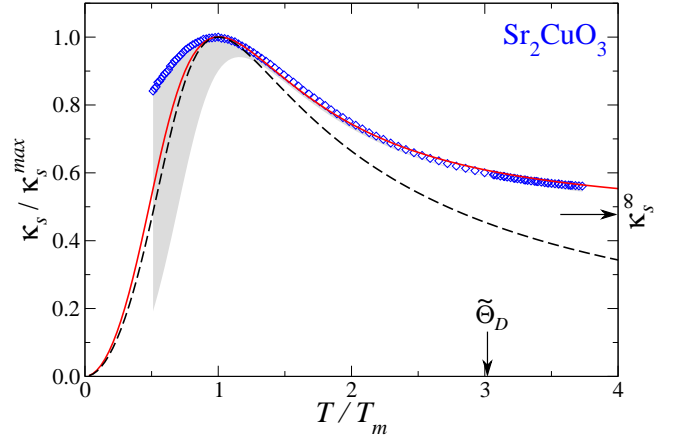


FIG. 4: Spin thermal conductivity κ_s normalized to its maximal value vs reduced temperature T/T_m . Diamonds are the experimental data for Sr_2CuO_3 , Ref. 5. $T_m = 79.4\text{K}$ and $\kappa_s^{max} = 36.7\text{Wm}^{-1}\text{K}^{-1}$ for this material. Shaded area schematically represents the range where the phonon background subtraction creates a large uncertainty in the data.⁵ Solid line is the results of this work, Eq. (51), for $\Theta_D = 11.6T_m$. Arrows mark the saturation value κ_s^∞ for the solid line at $T \gg \tilde{\Theta}_D$ and the spin-phonon scattering crossover scale $\tilde{\Theta}_D$. Dashed line corresponds to $\kappa_s(T)$, Eq. (51), for $\Theta_D \rightarrow \infty$. [These results were recently presented in Ref. 39.]

We would like to emphasize that apart from κ_s^{max} and T_m there is only one adjustable parameter, Θ_D , which is used in our fitting procedure, and yet our theory yields an excellent agreement with the experimental data over the whole temperature range.

Note that the transition between intermediate- and high-temperature regimes for κ_s is determined by the scale $\tilde{\Theta}_D$, which separates different temperature behavior for the spin-phonon scattering as discussed in Sec. III. It is this scale, not the Debye temperature itself, is a parameter of our theory. For Sr_2CuO_3 this scale is found to be $\tilde{\Theta}_D \approx 3T_m = 240\text{K}$, shown in Fig. 4 by an arrow.

The value of the Debye temperature Θ_D that comes out from our fit of thermal conductivity for Sr_2CuO_3 is $\Theta_D = 11.6T_m \approx 900\text{K}$, which is higher than the estimations of Θ_D for this material obtained by a different method.⁵ Since in our theory the Debye temperature is a characteristic energy scale for the phonon bandwidth this may imply that the spin system is also coupled to the optical phonons. In fact, the typical width of the whole phonon spectra in the cuprates is about 900K.⁵⁴

To complete our comparison we provide here the asymptotic expressions for $\kappa_s(T)$ in the low- and intermediate-temperature regimes. At small temperature $T_{\text{KF}} \ll T \ll T_m$ the thermal conductivity is:

$$\frac{\kappa_s(T)}{\kappa_s^{max}} = \frac{\pi^2\gamma_1}{3\gamma_2} \frac{T^2}{T_m^2} \approx 2.26 \frac{T^2}{T_m^2}. \quad (53)$$

In this regime the conductivity is controlled entirely by impurities.

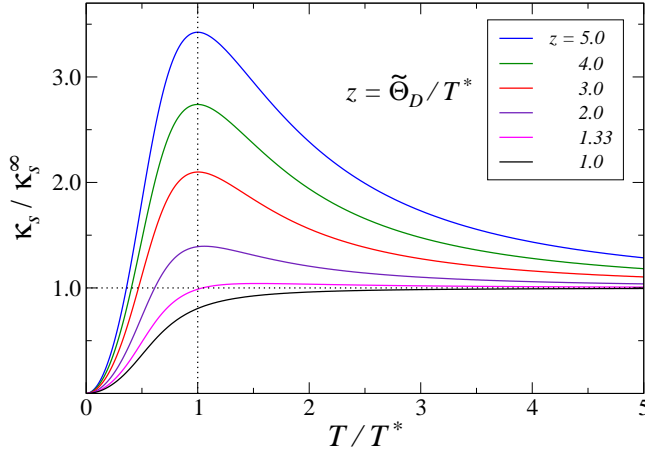


FIG. 5: Spin thermal conductivity κ_s normalized to its value at ∞ vs reduced temperature T/T^* for various values of $z = \tilde{\Theta}_D/T^*$. (z decreases from the top to the bottom curve).

When the temperature is higher the number of high-energy spin bosons increases. The most important relaxation mechanism for these excitations is the spin-phonon scattering. However, the low-energy spin bosons are still scattered mostly by impurities. Thus, at intermediate temperature $T_m \ll T \ll \tilde{\Theta}_D$ both mechanisms contribute to the relaxation of the thermal current:

$$\frac{\kappa_s(T)}{\kappa_s^{max}} = \frac{\pi\gamma_1}{2\sqrt{\gamma_2}} \frac{T_m}{T} \approx 1.46 \frac{T_m}{T}. \quad (54)$$

These asymptotic formulas can be tested experimentally, although the intermediate-temperature regime for Sr_2CuO_3 is not very well pronounced because $\tilde{\Theta}_D$ is only 3 times larger than T_m . Such an intermediate asymptotic behavior might be more relevant for some other systems where the difference between T_m and $\tilde{\Theta}_D$ is larger.

For larger temperatures $T > \tilde{\Theta}_D$ the thermal conductivity saturates. Thus, one of the most straightforward ways to verify our theory would be to measure the thermal conductivity for higher temperatures and check if the saturation really takes place as we predict.

Different choices of Θ_D . One may wonder at this point how much variation in the temperature dependence of κ_s can be expected from the theory given by Eq. (48) or (51) if the parameters of the model, such as Θ_D , are varied. As is mentioned above there are three independent parameters: phonon- and impurity-couplings \mathcal{A} and Δ , and the Debye temperature Θ_D . To generate a sequence of curves for the theoretical κ_s v.s. T the following procedure is convenient. Since at $T \gg \Theta_D$ thermal conductivity given by Eq. (48) saturates at a constant value, it is convenient to normalize $\kappa_s(T)$ to its value at $T = \infty$, i.e. κ_s^∞ , not to κ_s^{max} . This is also because for $\tilde{\Theta}_D \lesssim 1.25$ $\kappa_s(T)$ becomes a monotonic function and the determination of κ_s^{max} is ambiguous. Such a normalization reduces the number of free parameters to two. It is natural to choose one of those parameters to be a phonon crossover

scale $\tilde{\Theta}_D (\simeq \Theta_D/4)$ and to define the other one as a reference temperature T^* . Using Eq. (51) with dimensionless constants γ_1 and γ_2 related through:

$$1 = \frac{\pi\gamma_1}{2\sqrt{\gamma_2}} \frac{T^*}{\tilde{\Theta}_D}, \quad (55)$$

one can generate a sequence of curves for κ_s/κ_s^∞ v.s. $t = T/T^*$ for various values of $z = \tilde{\Theta}_D/T^*$ shown in Fig. 5. Results for $z = 5, 4, 3, 2, 1.33$, and 1 are shown (z decreases from the top to the bottom curve). The value of $\gamma_2 = 1.83$, same as in Fig. 4, is used to ensure that for $\tilde{\Theta}_D \gg T^*$ (in reality, for $\tilde{\Theta}_D \gtrsim 2T^*$) the reference temperature automatically corresponds to the temperature of the maximum, i.e. $T^* \equiv T_m$. Different choice of γ_2 would simply correspond to rescaling of T^* leaving the form of $\kappa_s(t)$ unchanged. Thus, Fig. 5 gives a description of possible variations in the results of the theory given by Eq. (48) within the experimentally relevant range of Θ_D/T^* .

As is described above, in order to fix the remaining two parameters and fit the experimental data one may associate the experimental value of T_m with the position of the theoretical maximum and then vary $\tilde{\Theta}_D$ to match $\kappa_s^{max}/\kappa_s^\infty$, for example. A similar strategy has been used to obtain Fig. 4 where the best fit closely corresponds to $z = 3$ curve in Fig. 5. If the experimental curve does not have a maximum,⁵⁵ one can choose any other reasonably distinct $\kappa_s(T')$ in order to fix the choice of theoretical parameters T^* and $\tilde{\Theta}_D$.

Origin of T_m . The temperature T_m at which κ_s reaches its maximum can be expressed through the original parameters of the problem as:

$$T_m = \left(\frac{v^5 \Delta^2}{\gamma_2 \mathcal{A}} \right)^{1/6} \propto v \left(\frac{n\delta J_{\text{imp}}^2}{v\mathcal{A}} \right)^{1/6}. \quad (56)$$

In a similar fashion one can relate κ_s^{max} to the microscopic parameters as:

$$\kappa_s^{max} = \frac{v^6}{\gamma_1 \pi \mathcal{A} T_m^4} \propto \frac{v^2}{\mathcal{A}} \left(\frac{v\mathcal{A}}{n\delta J_{\text{imp}}^2} \right)^{2/3}. \quad (57)$$

The physical meaning of T_m is the following. It is possible to define the “thermal” spin-phonon relaxation rate:

$$\frac{1}{\tau_{sp}^T} = \frac{1}{\tau_{sp}(k)} \Big|_{k=k_T} = \frac{\mathcal{A} T^5}{v^5}, \quad (58)$$

where $k_T = T/v$. By its definition τ_{sp}^T is independent of k . It characterizes rate of the spin-phonon collisions of the thermal spin bosons at a given temperature. The scale T_m emerges naturally as a solution of the equation:

$$\tau_{sp}^T = \tau_{\text{imp}}. \quad (59)$$

In other words, when $T \propto T_m$ the thermal spin-phonon and spin-impurity collision rates are the same. At the

temperature higher (lower) than T_m the spin-phonon (impurity) scattering dominates. Note that in the low-temperature regime we assume that the temperature is still much larger than the Kane-Fisher temperature T_{KF} .

Origin of κ_s^∞ . Our work predicts a remarkable behavior of the thermal conductivity at the temperatures higher than the scale related to the Debye energy: saturation at a constant value, Eq. (52). A parallel can be drawn with the thermal conductivity of metals, where the electronic part of κ saturates at the temperatures above the Debye energy.⁴⁵ The parallel can be suspected to be even deeper because of the presence of the large energy scales in both problems, Fermi energy $E_F \gg T$ in the case of metals and $J \gg T$ in our case.

A closer examination, however, reveals a difference between the two cases. In metals, the thermal conductivity temperature behavior is defined by the electronic specific heat $C_e(T)$ and the electron-phonon relaxation time $\tau_{ep}(T)$ through the quasichlassical relation: $\kappa_e(T) = C_e(T)v_F^2\tau_{ep}(T)/3$. Note that it is the thermalized electrons which contribute most substantially to the transport. Specific heat is linear in T , while at $T \gtrsim \Theta_D$ the relaxation time is inversely proportional to the temperature due to the thermal population of phonons, $\tau_{ep}(T) \propto 1/T$. Altogether, this renders $\kappa_e = \text{const}$.

In our case the excitations are spin bosons, not fermions at large momentum k_F . Therefore, in contrast, in the phonon-scattering dominated regime $T \gg T_m$ the spin-boson relaxation rate is strongly k -dependent and the major contribution to the thermal current comes from the long-wavelength bosons with $k \ll T/v$. Thus, the impurity-scattering continues to contribute to the temperature dependence of the thermal conductivity at higher temperatures. Therefore, in the case of spin chains the saturation of κ_s is a result of a non-trivial combination of: particular temperature- and k -dependencies of the impurity and phonon relaxation rates and the 1D density of states of the spin-bosons.

Further predictions. Our equations (52), (56) and (57) allow us to formulate several predictions of our model for the impurity concentration dependence of several quantities that can be verified experimentally.

First, we see that the temperature T_m at which $\kappa_s(T)$ reaches its maximum scales as $n^{1/6}$. Such a weak dependence means that for a particular material the maximum in κ_s should be around the same temperature for a broad range of disorder concentration.

Second, the maximum value of the thermal conductivity $\kappa_s^{\text{max}} = \kappa_s(T_m)$ scales as $n^{-2/3}$, Eq. (57). Third, the saturation value κ_s^∞ has yet different concentration dependence $n^{-1/2}$. Such behaviors can be looked for in the materials with the isotope substitution for either magnetic ions (Cu^{2+}) or surrounding ions as they all will lead to the local modification of the superexchange constant. If such dependencies are observed this will provide strong support to our theory.

Another interesting experimental suggestion is based on the specifics of the spin-phonon scattering which we

have found in Sec. III. Namely, the most important scattering of spin bosons in the phonon-dominated regime is due to phonons whose momentum is almost normal to the direction of the spin chains. The characteristic energy of such phonons is T . One can think of the following experimental setup: the heat current is directed along the chains while the thermal phonon pulse is induced perpendicular to the heat current (e.g., by a short laser pulse). This should lead to a sizable suppression of the spin-boson thermal current due to additional scattering by the extra phonons. The increase of the phonon heat current due to transverse pulse will be either negligible or can be accounted for by comparing to the results of the same experiment with the heat current and heat pulse both directed perpendicular to the chains.

Consistency check. In considering the spin-boson relaxation due to phonons we emphasized the importance of the two-stage, bottle-neck process, in which the spin boson scatters on the phonon via a “normal” process, while the momentum relaxation via an Umklapp process is taken care of by the phonon bath. Having carried out a comparison with experiments we can now verify the consistency of our results with the initial assumption. Namely, we can now check whether the characteristic spin-phonon relaxation time τ_{sp} is indeed much longer than the characteristic phonon-phonon relaxation time τ_{pp} .

Since below T_m the scattering is impurity-dominated we need to estimate the relaxation times for $T \geq T_m$ only. We have already introduced the “thermal” relaxation time for spin bosons τ_{sp}^T in Eq. (58). At $T = T_m$ one can express such relaxation time through κ_s^{max} , Eq. (57), as:

$$\tau_{sp}^T = \frac{\gamma_1 \pi \kappa_s^{\text{max}}}{v T_m}. \quad (60)$$

The phonon relaxation time can be estimated from the quasichlassical expression for the phonon thermal conductivity: $\kappa_{ph} = c^2 C(T_m) \tilde{\tau}_{pp}/3$, where $C(T_m)$ is the lattice specific heat and $\tilde{\tau}_{pp}$ is the average transport relaxation time of a phonon due to phonon-phonon scattering.

Using these expressions we write the ratio of the thermal spin-phonon and the average phonon-phonon relaxation times as:

$$\frac{\tau_{sp}^T}{\tilde{\tau}_{pp}} = \gamma_1 \left(\frac{C(T_m)}{3} \right) \left(\frac{\kappa_s^{\text{max}}}{\kappa_{ph}} \right) \left(\frac{c}{v} \right) \left(\frac{\Theta_D}{T_m} \right), \quad (61)$$

where the specific heat $C(T_m)$ can be found as $\min\{3; 12\pi^2(T_m/\Theta_D)^3/5\}$.⁴³ One can see that the smallness of c/v in (61) is canceled by the largeness of Θ_D/T_m . For Sr_2CuO_3 in the region around T_m the spin-boson and phonon parts of the thermal conductivity are of the same order. Also, $C(T_m) \approx 2$. Taking the actual values of κ_s^{max} , κ_{ph} , T_m , J , etc. for Sr_2CuO_3 we find that: $\tau_{sp}^T/\tilde{\tau}_{pp} \simeq 0.5 \div 1$.

It appears, superficially, that our assumption is not valid. However, at $T > T_m$ the typical momentum \tilde{k}

of a spin boson contributing to the thermal transport is much smaller than the “thermal” momentum $k_T = T/v$: $\tilde{k}/k_T \approx (T_m/T)^3$. Thus, the typical relaxation time is much larger than the thermal one $\tau_{sp} \approx \tau_{sp}^T \cdot (k_T/\tilde{k})^2$. We also recall here that the phonons contributing to our two-stage process most effectively are the thermalized phonon with the momentum $P_T \sim T/c$ as shown in Sec. III. Therefore, τ_{pp}^T of such a phonon is much shorter than the average transport relaxation time $\tilde{\tau}_{pp}$ which we estimated above, $\tau_{pp}^T \ll \tilde{\tau}_{pp}$. Thus, the characteristic spin-phonon and phonon-phonon times involved in the two-stage process obey:

$$\frac{\tau_{sp}}{\tau_{pp}^T} \gg \frac{\tau_{sp}^T}{\tilde{\tau}_{pp}} \approx 1, \quad (62)$$

due to both $\tau_{sp} \gg \tau_{sp}^T$ and $\tau_{pp}^T \ll \tilde{\tau}_{pp}$. This proves the validity of our approach.

We also estimated the Kane-Fisher temperature for Sr_2CuO_3 from

$$\kappa_s^{max} \approx \frac{aT_m^2}{nT_{KF}}, \quad (63)$$

which follows from Eqs. (38), (56), and (57). Using experimental values for κ_s^{max} and T_m one obtains that

$$\frac{T_{KF}}{T_m} \approx 10^{-3} n^{-1}, \quad (64)$$

which means that our assumption for the impurity-controlled regime $T_{KF} \ll T_m$ is valid unless the impurity concentration n is less than 0.1%. We are not aware of the actual level of disorder in Sr_2CuO_3 , but such a high purity is unlikely. Therefore, this assumption is valid too.

With the help of our asymptotic formula (57) one can estimate the spin-coupling constant using experimental values of κ_s^{max} and T_m . This estimate leads to an unreasonably high value of $\mathcal{A}/Ja^5 \sim 10^4$. First, a large value of the spin-phonon coupling constant can be due to an exponential dependence of the superexchange on the interatomic distance, as it is generated by the virtual tunnelling of electrons. Second, as one can see from Eqs. (56) and (57) the expression for the spin-phonon coupling contains high powers of both J and T_m . This creates an extra sensitivity of the result of our estimate to the unknown dimensionless constants, which our theory might be unable to capture.⁵⁶

Other materials. Other materials of the cuprate family in which the anomalous thermal transport has been observed include the zig-zag chain⁵ and spin-ladder materials,¹ and another spin-chain material, $\text{BaCu}_2\text{Si}_2\text{O}_7$, with much smaller superexchange constant.⁷

The most straightforward case for applying our theory seems to be the case of SrCuO_2 where the spin excitation spectrum remains gapless because of the frustrated coupling between the chains. Since the inter-chain coupling is of order $J'/J \sim 0.1$ one may expect that while the low-

and intermediate- T behavior of κ_s should be the same as in the case of Sr_2CuO_3 , the high- T part might be different due to an additional scattering mechanism from the inter-chain interaction. However, as we show in Section VI, the high- T regime is fully dominated by the long-wavelength spin excitations, which means that J' should remain irrelevant and the behavior of $\kappa_s(T)$ for SrCuO_2 should be very similar to the “simple” chain material Sr_2CuO_3 at all temperatures. Nevertheless, we were unable to fit the experimental data for SrCuO_2 ⁵ as successfully as for Sr_2CuO_3 . On the other hand, as we learned from a very recent work Ref. 55 there might be an issue with the subtraction background for these materials. The thermal conductivity of the 5% Ca-doped SrCuO_2 does exhibit a saturation at high-temperatures, in an excellent agreement with our theory, but the peak at lower temperatures is much less pronounced. We therefore refrain from an explicit comparison of our theory to SrCuO_2 until the experimental issues are settled.

In the case of $(\text{La,Ca,Sr})_{14}\text{Cu}_{24}\text{O}_{41}$ materials the excitations are gapped. Therefore, the results of our work cannot be straightforwardly applied to them because the gap, not the impurity scattering, controls the low-energy cut-off scale. Thus, one needs to reconsider the problem of the thermal transport for the gapped spin systems. On the other hand, the spin-phonon scattering part of such a consideration may stay very similar to our case, especially for $\text{Ca}_9\text{La}_5\text{Cu}_{24}\text{O}_{41}$. This latter compound presumably contains a lot of 3D disorder (not related to the spin subsystem) due to a random distribution of Ca and La ions,¹ which might help to facilitate the fast phonon momentum relaxation and ensure that $\tau_{pp} \ll \tau_{sp}$ at high temperatures. We would like to note that another very recent experimental work, Ref. 57, has discussed the role of the spin-phonon coupling in the gapped systems using a very different framework.

The case of another spin-chain material, $\text{BaCu}_2\text{Si}_2\text{O}_7$, is also different because of the lack of the spin and lattice energy scales separation. In this compound the spin boson velocity is of the same order as the sound velocity, $v \approx c$.⁷ Therefore, the kinematic considerations of our work will not be applicable for the collision integral in this system. In the temperature regime $T \sim J$, easily achievable for this material, the thermal transport will be influenced by various other relaxation processes, which are negligible in our case.

Altogether, the differences in the underlying spin models for some of these materials will, most certainly, lead to different temperature behaviors of κ_s . Therefore, a detailed microscopic study in these systems along the lines of our work is necessary.

VI. MEAN FREE PATH

Having described successfully the temperature dependence of the thermal conductivity in Sr_2CuO_3 we would like to discuss the length scales that characterize scat-

tering in this system. We also would like to address the question of whether the concept of the mean free path can be applied to describe thermal conductivity by spin bosons. More specifically, we would like to ask whether the thermal conductivity of spin bosons can be written in a simplified form (sometimes referred to as the simple kinetic equation):

$$\kappa_s(T) = v C_s(T) \bar{\ell}(T), \quad (65)$$

and if yes in what regime. Here $C_s(T)$ is the specific heat of the spin chains and $\bar{\ell}(T)$ is the mean free path.

In the end, we also verify that the wavelength of a typical excitation contributing to the thermal current in Sr_2CuO_3 is shorter than its mean free path. This condition is needed for the applicability of the Boltzmann equation formalism (quasiclassical approximation).

The “total” relaxation time of the spin boson with the wave-vector k is defined in Eq. (45). Thus, one can introduce corresponding k - and T -dependent length scale:

$$\ell(k, T) = \frac{v}{\tau_{\text{imp}}^{-1}(T) + \tau_{\text{sp}}^{-1}(k, T)}. \quad (66)$$

In order to be clear on terminology we would like to refer to this k -dependent length scale as to the “ k -dependent mean free path” of the spin boson. At the same time the notion “mean free path” will be reserved for an averaged, only T -dependent, length scale.

Cut-off length. Spin-phonon scattering rate in Eq. (66) depends on k as $\tau_{\text{sp}}^{-1} \propto k^2$ while impurity scattering rate is k -independent and plays the role of a cut-off scale. Therefore, it is natural to introduce the “cut-off” length as:

$$\ell_{\text{imp}}(T) \equiv \ell(0, T) = \frac{vT}{\Delta^2}, \quad (67)$$

using explicit expression for τ_{imp}^{-1} , Eq. (43). It is interesting to find out the absolute value of such a length for the real system like Sr_2CuO_3 . Since all the impurity- and phonon-related parameters, Δ , \mathcal{A} , and $\tilde{\Theta}_D$, have been related to the phenomenological constants T_m ($\simeq 80\text{K}$) and κ_s^{max} ($\simeq 37 \text{ W m}^{-1}\text{K}^{-1}$), one can re-express Δ through them and obtain:

$$\ell_{\text{imp}}(T) = \frac{\pi\gamma_1}{\gamma_2} \frac{\hbar\kappa_s^{\text{max}} b c}{k_B^2 T_m \sqrt{2}} \frac{T}{T_m} \simeq 300a \frac{T}{T_m}, \quad (68)$$

where $a = 3.9\text{\AA}$ and $b = 3.5\text{\AA}$ and $c = 12.7\text{\AA}$ are the lattice constants along and perpendicular to the chains in Sr_2CuO_3 , respectively.⁴¹ Such a large value of ℓ_{imp} ($\approx 1200\text{\AA}$ at $T = T_m$) is in agreement with the estimates for the mean free path made in the experimental works.^{5,6} Note that the cut-off length *grows* as the temperature increases. This is a consequence of the impurity scattering in 1D spin-chains which is non-perturbative in the number of spin bosons.

k -dependent mean free path. We now express the k -dependent mean free path (66) through the cut-off length

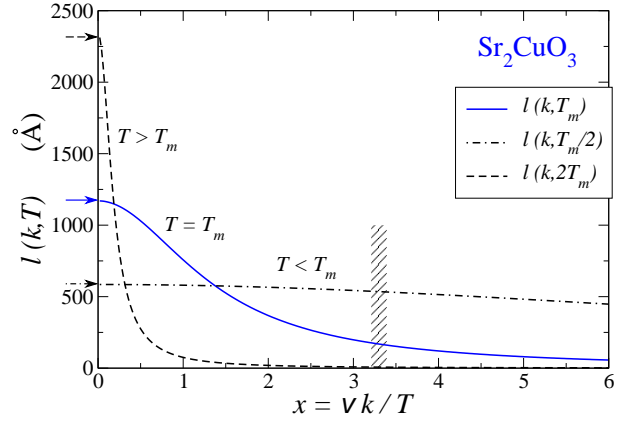


FIG. 6: k -dependent mean free path $\ell(k, T)$ v.s. $x = vk/T$ for three representative temperatures: $T = T_m$ (solid), $T = T_m/2$ (dot-dashed), and $T = 2T_m$ (dashed). Arrows mark the cut-off length $\ell_{\text{imp}}(T)$ for each temperature. An approximate boundary of the bosonic thermal population is marked by the shaded area.

(67) using the explicit form of the spin-phonon scattering rate, Eq. (30):

$$\frac{\ell(k, T)}{\ell_{\text{imp}}(T)} = \left[1 + \frac{1}{\gamma_2} \left(\frac{vk}{T} \right)^2 \left(\frac{T}{T_m} \right)^6 \Gamma \left(\frac{\tilde{\Theta}_D}{T} \right) \right]^{-1}, \quad (69)$$

where $\Gamma(\tilde{\Theta}_D/T)$ is the auxiliary crossover function introduced in Eq. (31), which is related to the Debye temperature: $\Gamma \approx 1$ for $T < \tilde{\Theta}_D$ and $\Gamma \approx (\tilde{\Theta}_D/T)^2$ for $T > \tilde{\Theta}_D$. Our Fig. 6 shows the k -dependent mean free path $\ell(k, T)$ v.s. $x = vk/T$ for three representative temperatures: $T = T_m$ (solid), $T = T_m/2$ (dot-dashed), and $T = 2T_m$ (dashed). From Eq. (69) one can see that $\ell(x, T)$ is a Lorentzian with the height given by the cut-off length $\ell_{\text{imp}}(T)$ (marked by arrows in Fig. 6) and a temperature-dependent width. This width depends on T quite strongly: $\propto T^{-3}$ for $T < \tilde{\Theta}_D$ and $\propto T^{-2}$ for $T > \tilde{\Theta}_D$.

The spin boson energy normalized by to the temperature $x = vk/T$ is a natural variable to describe thermal processes. The values of x which are of significance for such processes are $\lesssim 3$ because of the bosonic thermal population; this boundary is marked by the shaded area in Fig. 6. One can see that the k -dependent mean free path is essentially constant for $x < 3$ in the impurity-dominated regime $T = T_m/2$, while it depends on x very strongly in the phonon-dominated regime $T = 2T_m$.

Impurity-dominated regime. Already from this observation one can see that in the impurity-dominated regime all the spin bosons involved in the thermal transport are characterized by approximately the same mean free path $\ell(k, T) \approx \ell_{\text{imp}}(T)$, Fig. 6 dash-dotted line, and thus the mean free path concept readily applies here. Namely, one can re-write our expression for the thermal conductivity, Eq. (48), somewhat differently, using the k -dependent

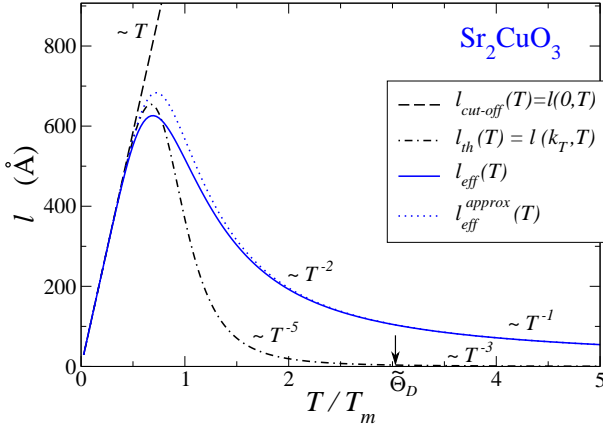


FIG. 7: The temperature dependence of the cut-off length $\ell_{\text{imp}} (\propto T$, dashed) and the “thermal” length $\ell_{th}(T) = \ell(T/v, T)$ (dashed-dotted). In the phonon-dominated regime $\ell_{th}(T) \propto T^{-5}$ for $T < \tilde{\Theta}_D$ and $\propto T^{-3}$ for $T > \tilde{\Theta}_D$. The “effective” mean free path $\ell_{eff}(T)$, Eq. (75), and the approximate “effective” mean free path $\ell_{eff}^{app}(T)$, Eq. (76), are also shown (solid and dotted, respectively).

mean free path from Eqs. (66) and (69):

$$\kappa_s(T) = \frac{T}{\pi} \int_0^\infty \frac{x^2 e^x}{(e^x - 1)^2} \ell(x, T) dx. \quad (70)$$

Since $\ell(x, T)$ is x -independent in the impurity-dominated regime, this expression can be reduced to the form (65)

$$\kappa_s(T) = v C_s(T) \ell_{\text{imp}}(T), \quad (71)$$

with the mean free path equal to the cut-off length $\bar{\ell}(T) \equiv \ell_{\text{imp}}(T)$, Eq. (68), and the specific heat given by:

$$C_s(T) = \int_k v |k| \left| \frac{\partial f_k}{\partial T} \right| = \frac{T}{\pi v} \int_0^\infty \frac{x^2 e^x dx}{(e^x - 1)^2} = \frac{2}{3} \frac{T}{Ja}, \quad (72)$$

where $v = \pi J/2$ and the well-known value of the integral ($= \pi^2/3$) have been used. Thus, our result for the mean free path in the low- T regime ($T < T_m$) is $\ell \propto T$, which disagrees with experimental works where often a constant mean free path at low temperatures is reported.^{6,7} However, this is the regime where experimental data for the spin part of the thermal conductivity are unreliable due to large phonon background.

Phonon-dominated regime. One can see from Fig. 6 that the situation for $\ell(x, T)$ is quite different in the phonon-dominated regime. While the cut-off length grows as the temperature increases, the range of the energies of the spin bosons effectively participating in the thermal transport shrinks. In fact, it is a very unusual feature of the problem: as the temperature increases the thermal current becomes dominated by the excitations with longer and longer wavelengths. Therefore, our approximations related to spin excitations, such as the use of bosonization language, become better justified for higher temperatures.

Using Eq. (69) one can define the “typical” momentum of the spin boson \tilde{k} , corresponding to the width of the Lorentzian $\ell(\tilde{k}, T) = \ell_{\text{imp}}/2$:

$$\begin{aligned} \tilde{k} &\approx \frac{T_m}{Ja} \left(\frac{T_m}{T} \right)^2 \approx \frac{1}{20a} \left(\frac{T_m}{T} \right)^2 \quad \text{for } T < \tilde{\Theta}_D, \\ \tilde{k} &\approx \frac{T_m}{Ja} \frac{T_m}{\tilde{\Theta}_D} \frac{T_m}{T} \approx \frac{1}{60a} \frac{T_m}{T} \quad \text{for } T > \tilde{\Theta}_D \end{aligned} \quad (73)$$

where the values $J/T_m = 20$ and $\tilde{\Theta}_D/T_m = 3$ for Sr_2CuO_3 were used.

Evidently, at $T > T_m$ one cannot possibly assume that all the spin-boson excitations are characterized by the same k -dependent mean free path. Therefore, one cannot reduce Eq. (70) for $\kappa_s(T)$ to a simplified form, Eq. (65). In other words, the mean free path concept cannot be, strictly speaking, applied to the phonon-dominated regime of the problem. This is further demonstrated in our Fig. 7 which shows the temperature dependence of the cut-off length $\ell_{\text{imp}} (\propto T$, dashed) and the “thermal” length $\ell_{th}(T) = \ell(T/v, T)$ (k -dependent mean free path for the excitation with the energy $= T$, dashed-dotted). The latter length, while indistinguishable from the cut-off length in the impurity-dominated regime $T < T_m$, dies off very quickly in the phonon-dominated regime $T > T_m$ (as $\propto T^{-5}$ for $T < \tilde{\Theta}_D$ and then as $\propto T^{-3}$ for $T > \tilde{\Theta}_D$). This is simply to reiterate our point that the spin bosons are characterized by strongly k -dependent mean free paths for $T > T_m$.

“Effective” mean free path. Nevertheless, one may want to insist on using the simplified equation (65) in order to extract some “effective” mean free path $\ell_{eff}(T)$ characterizing the system, an approach used in the experimental works,^{5,6}

$$\kappa_s(T) \stackrel{\text{def}}{=} v C_s(T) \ell_{eff}(T). \quad (74)$$

Using the explicit form of $C_s(T)$ obtained above (72) the “effective” mean free path $\ell_{eff}(T)$ can be written as:

$$\ell_{eff}(T) \stackrel{\text{def}}{=} \frac{3}{\pi^2} \int_0^\infty \frac{x^2 e^x}{(e^x - 1)^2} \ell(x, T) dx. \quad (75)$$

This integral can be taken numerically and $\ell_{eff}(T)$ is plotted in Fig. 7 (solid line). Note again that all three lengths, $\ell_{\text{imp}}(T)$, $\ell_{th}(T)$, and $\ell_{eff}(T)$ are indistinguishable for $T < T_m$ while they are very different for $T > T_m$.

Recalling that the height of the Lorentzian $\ell(x, T)$ grows $\propto T$ while the width is decreasing $\propto T^{-3}$ for $T < \tilde{\Theta}_D$ and $\propto T^{-2}$ for $T > \tilde{\Theta}_D$ one can immediately conclude that $\ell_{eff}(T)$ should decay as $\propto T^{-2}$ for $T < \tilde{\Theta}_D$ and $\propto T^{-1}$ for $T > \tilde{\Theta}_D$ as marked in Fig. 7. Since $C_s(T) \propto T$, this yields $\kappa_s \propto \text{const}$ behavior for $T > \tilde{\Theta}_D$.

Using the fact that the width of $\ell(x, T)$ is strongly T -dependent one can obtain an approximate expression for $\ell_{eff}(T)$ in Eq. (75) which is valid in both asymptotic limits $T \ll T_m$ and $T \gg T_m$:

$$\ell_{eff}^{app}(T) = \frac{\ell_{\text{imp}}(T_m)}{Bt^2 \sqrt{\Gamma(t)}} \arctan(Bt^3 \sqrt{\Gamma(t)}), \quad (76)$$

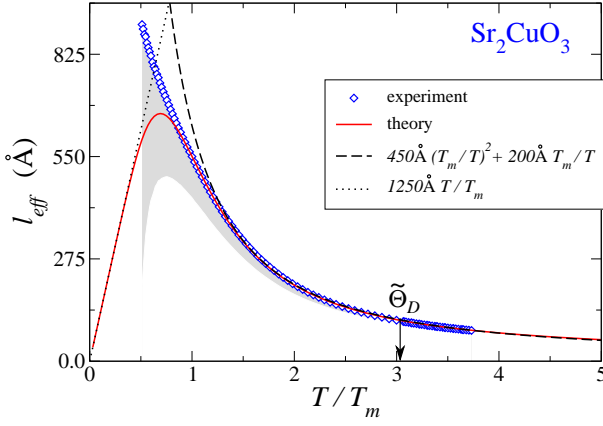


FIG. 8: The “effective” mean free path, Eq. (75), compared to the experimental results of Refs. 4,5. Asymptotic fits $\propto T$ for $T < T_m$ and $\propto 1/T + C/T^2$ for $T > T_m$ are shown by the dashed lines. Shaded area schematically represents the experimental error bars due to the phonon subtraction.

where $t = T/T_m$ and constant $B = 2.5$. It is shown in Fig. 7 (dotted line). Using explicit form of $\Gamma(\tilde{\Theta}_D/T)$ one can obtain all the correct asymptotic behaviors of $\ell_{eff}(T)$ from it.

Our Fig. 8 shows our “effective” mean free path, Eq. (75), compared to the same quantity derived in Refs. 5,6 from the experimentally measured $\kappa_s(T)$ using Eq. (74). Asymptotic fits $\propto T$ for $T < T_m$ and $\propto 1/T + C/T^2$ for $T > T_m$ are also shown. Shaded area schematically represents the experimental error bars due to the phonon subtraction.

Saturation in κ_s and parallel with metals. We would like to return to the discussion of the origin of saturation in $\kappa_s(T)$ at $T > \tilde{\Theta}_D$. One may be surprised, once again, by the seemingly identical features of the high- T thermal conductivity in both the spin chains and metals: (i) in both cases there is large scale (E_F and J , respectively) which yields “fast” excitations, (ii) in both cases specific heat $\propto T$ up to very high temperatures, (iii) for the saturation regime the dominant scattering is due to phonons in both cases, (iv) mean free path for metals and “effective” mean free path for spin bosons are $\propto 1/T$ in this regime.

It is very tempting to conclude that in the case of the spin chains the $1/T$ behavior in the “effective” mean free path is due to phonon population $n_{ph} \propto T$ as in the case of metals. However, it is much more subtle in this case. As we discussed above and in previous Section, thermal transport in spin chains relies on the long-wavelength bosons, even more so for the high temperatures (see Fig. 6), and the T -dependence of the impurity scattering remains important. Simply put: if the impurity scattering would provide ℓ_{imp} v.s. T different from $\propto T$, the T -dependence of the ℓ_{eff} would be different from $\propto 1/T$ and there would be no saturation in $\kappa_s(T)$. In fact, this seems to be the case for the related frustrated ladder (zig-zag chain) material SrCuO_2 , which has gapless ex-

citations as in spin chains, but its thermal conductivity does not seem to saturate at higher T .⁵

Once again, it is an interesting and unusual situation in spin chains: it is always the long-wavelength range of excitations which is crucial for the thermal transport, temperature increase only enhances the phonon scattering and shrinks the relevant energy region for spin bosons. Thus, our results are universal and do not depend on the manner in which bosonization or other approximations break down at higher energies.

Quasiclassical approximation. It is instructive to verify the validity of the quasiclassical approximation which is implicitly used when utilizing Boltzmann equation for the lower-order scatterings. One needs to show for the “typical” spin boson that its wavelength $\tilde{\lambda}$ is shorter than its k -dependent mean free path $\tilde{\lambda} < \tilde{\ell}$.

$T > T_m$ case. Consider $T > T_m$ first. We have already defined the “typical” momentum for this case in Eq. (73). Using $J/T_m = 20$ and $\tilde{\Theta}_D/T_m = 3$ specific for Sr_2CuO_3 we find (neglecting numerical coefficients of order one):

$$\begin{aligned} \tilde{\lambda} &\sim \frac{Ja}{T_m} \left(\frac{T}{T_m} \right)^2 \approx 20a \left(\frac{T}{T_m} \right)^2 \quad \text{for } T < \tilde{\Theta}_D, \\ \tilde{\lambda} &\sim a \frac{J}{T_m} \frac{\tilde{\Theta}_D}{T_m} \frac{T}{T_m} \approx 60a \frac{T}{T_m} \quad \text{for } T > \tilde{\Theta}_D. \end{aligned} \quad (77)$$

The “typical” k -dependent mean free path is defined as:

$$\tilde{\ell} \equiv \ell(\tilde{k}, T) \equiv \frac{\ell_{imp}(T)}{2} \approx 150a \frac{T}{T_m}. \quad (78)$$

Therefore, $\tilde{\ell} > \tilde{\lambda}$ is always fulfilled for the phonon-dominated regime.

$T < T_m$ case. In the impurity-dominated regime “typical” spin boson has an energy $v|k| \sim T$. Thus, the “typical” wavelength is:

$$\tilde{\lambda} \simeq a \frac{J}{T_m} \frac{T_m}{T} \approx 20a \frac{T_m}{T}. \quad (79)$$

The “typical” k -dependent mean free path is simply a cut-off length:

$$\tilde{\ell} = \ell_{imp}(T) \approx 300a \frac{T}{T_m}. \quad (80)$$

Thus, $\tilde{\ell} = \tilde{\lambda}$ at $T_b \approx T_m/4$ and the quasiclassical approximation is valid above this temperature.

VII. CONCLUSIONS

Approximations. We would like to review briefly the assumptions which have allowed us to solve the problem of spin-boson thermal transport in a reasonably simple analytical form.

The main assumption is the smallness of the phonon relaxation time as compared to the spin-phonon scattering time. This is justified since the spin-lattice coupling

is generically smaller than the phonon-phonon coupling. This also allows us to restrict ourselves with the lowest order in the spin-phonon coupling within the Boltzmann equation formalism. In addition, in our case $c \ll v$. Thus, at a given temperature the phonon population is much higher than that of the spin boson. This also implies higher relaxation rate for the phonons. If the above is true then the momentum relaxation of spin bosons can be viewed as a two-stage process with a bottle-neck. First, the momentum waits the longest time for a spin-boson-phonon collision to get transferred to the phonon subsystem. Second, the phonons quickly dissipate the transferred momentum. The first stage is the bottle-neck. Therefore, it controls the rate of the spin boson momentum dissipation. This is why we do not need to know microscopic details about the phonon-phonon collisions. It is enough to know that these collisions occur more often than the spin-boson scattering on the phonons.

The factor which might lead to violation of our assumption is exponential weakness of the phonon Umklapp relaxation at low enough temperatures. The Umklapp relaxation rate contains a characteristic exponent $e^{-b\Theta_D/T}$, b is a constant of order of unity.⁴³ Therefore, our approximation breaks down at very low temperature. Roughly speaking, this temperature corresponds to the point where the smallness of the spin-lattice coupling is comparable to the smallness of $e^{-b\Theta_D/T}$. In such a situation the bottle-neck scheme described above will cease to work and it will be necessary to include a detailed description of the phonon-phonon collisions as well. In practice, however, the impurity scattering will become relevant at much higher temperatures. Our theory shows a very weak impurity concentration dependence of the temperature below which impurities control the transport: $T_m \propto n^{1/6}$. This implies that even a very weak disorder will result in a substantial T_m .

We have verified our assumptions using the phenomenological parameters from the spin-chain material Sr_2CuO_3 and obtained that the two-stage process approximation is very well justified, see Sec. V.

We would like to note that the problem of the spin transport in spin chains coupled to 3D phonons has been studied within a different approach^{37,38} and gives a different temperature dependence for the spin thermal conductivity: $\kappa_s \propto \exp(T^*/T)$. The essential difference between our approaches is our treatment of the phonon bath as a source of the momentum dissipation. If this process is neglected the “Normal” transfer of the momentum from spins to phonons does not lead to degrading of the thermal current. Then, it is only the “direct” spin-phonon Umklapp processes which will be contributing to the transport relaxation rate with a characteristic exponential dependence on temperature. However, this could only work if the phonon system would be very reluctant to dissipate the momentum, which can only happen at the temperatures of the order of the “phonon peak” (30K for Sr_2CuO_3), well below the temperature of the maxi-

mum in the spin part of κ ($T_m = 80\text{K}$).

Final remarks. In this paper we have studied the problem of anomalous heat transport in quasi-1D spin-chain systems coupled to the 3D phonon environment in the presence of weak disorder. We have derived a microscopic model of 1D bosonic spin excitations interacting with phonons and impurities using bosonization approach. We have considered the spin-phonon scattering within the Boltzmann equation for the spin-boson distribution function. This equation has been solved in the limit of weak spin-lattice coupling and fast spin-boson excitations. Assuming that the phonon relaxation time τ_{pp} due to phonon-phonon scattering is much shorter than the spin-phonon relaxation time τ_{sp} we have obtained the transport relaxation rate for the spin bosons $\tau_{tr}^{-1} \approx \tau_{sp}^{-1} \propto k^2 T^3$ for $T \ll \Theta_D$ and $\propto k^2 T$ for $T \gtrsim \Theta_D$. We have shown that within our model the spin-phonon scattering alone is insufficient to render the thermal conductivity finite because the spin-phonon relaxation mechanism becomes ineffective for the spin bosons at low energies. On the other hand, the 1D impurity scattering provides a natural cut-off scale for the low-energy spin bosons and results in the momentum-independent scattering rate $\tau_{imp}^{-1} \propto T^{-1}$. Thus, the impurity scattering removes the divergence of the conductivity. We have calculated the thermal conductivity as a function of temperature and have shown that the low temperature transport is dominated by the impurity scattering while the high temperature transport is limited by both the impurity scattering and the spin-phonon collisions. Our main results are in a very good quantitative agreement with the available experimental data.

In implementing our approach we have also obtained an insight into various microscopic details of the problem. This has allowed us to formulate several predictions and suggest future experiments as well, see Sec. V. One of the predictions is the saturation of the spin-boson thermal conductivity at high temperatures: a non-trivial result due to impurity and spin-phonon scatterings and 1D nature of spin-bosons.

Further studies in the thermal conductivity of other spin systems using our approach are anticipated.

Acknowledgments

We would like to thank N. Andrei for useful conversations, E. Orignac for communications, and C. Yu for insightful comments which lead us to writing Sec. VI. We are also grateful to A. Sologubenko and C. Hess for sending experimental data. This work was supported by DOE under grant DE-FG02-04ER46174, and by the ACS Petroleum Research Fund. A.V.R. is grateful to the Dynasty Foundation of Dmitrii Zimin for support of this research.

APPENDIX A: SPIN-PHONON COLLISION INTEGRAL

In this Appendix we will present a detailed derivation of the relaxation time approximation for the spin boson collision integral.

The integral over \mathbf{P} in $S^{(1)}$, Eq. (25), can be evaluated explicitly. Let us denote the integrands of (25) other than delta-functions by $h(P_{\parallel}, \omega_{\mathbf{P}})$. Then, the integration over \mathbf{P} can be performed giving the following answer:

$$\int_{\mathbf{P}} \delta(\omega_{k'} + \omega_{\mathbf{P}} - \omega_k) \delta(k' + P_{\parallel} - k) h(P_{\parallel}, \omega_{\mathbf{P}}) = \frac{\omega_k - \omega_{k'}}{8\pi^3 c^2} h(k - k', \omega_k - \omega_{k'}) \theta(|k| - |k'|) \theta(x_0) \theta(\Theta_D^2 - x_0), \quad (\text{A1})$$

$$\text{with} \quad x_0 = v^2(|k| - |k'|)^2 - c^2(k - k')^2, \quad (\text{A2})$$

where $\theta(x)$ is a step function and Θ_D is the Debye temperature.

It is possible to act in the similar fashion for $S^{(2)}$ as well. The result of \mathbf{P} integration for this part of the collision integral differs by permutation of k and k' .

The step-functions θ in (A1) impose restrictions on the possible scattering states of the spin boson with the given momentum k . These restrictions are consequences of the conservation laws. Because of this step-functions the integration variable k' in Eqs. (25) and (26) for the collision integrals $S_{k\ell}^{(1,2)}$ is bound to an interval $\mathcal{C}_{\ell}^{(1,2)}$ smaller than the Brillouin zone. This interval, in general, depends on k . To find $\mathcal{C}_{\ell}^{(1)}$ we must solve:

$$0 < x_0 < \Theta_{D\ell}^2, \quad (\text{A3})$$

for $|k| > |k'|$. Graphical solution of these inequalities for $k > 0$ is presented in Fig. 9 as a lightly shaded area on (k, k') plane. In this Figure lines OA and OB are bisectors $k = \pm k'$. Although not shown in Fig. 9, $k < 0$ portion of the graphical solution can be obtained by an inversion of Fig. 9 with respect to the point O .

Equivalently, we can express the solution as the following choice of the integration interval $\mathcal{C}_{\ell}^{(1)}$ for $|k| > \Theta_{D\ell}/v$:

$$\mathcal{C}_{\ell}^{(1)} = \begin{cases} [k, k - \Theta_{D\ell}/v] \cup [-k + \sqrt{4(c_{\ell}/v)^2 k^2 + (\Theta_{D\ell}/v)^2}, -(1 - 2c_{\ell}/v)k] & \text{for } k > 0, \\ [-(1 - 2c_{\ell}/v)k, -k - \sqrt{4(c_{\ell}/v)^2 k^2 + (\Theta_{D\ell}/v)^2}] \cup [k + \Theta_{D\ell}/v, k] & \text{for } k < 0, \end{cases} \quad (\text{A4})$$

where we use $[k_{min}, k_{max}]$ to denote the interval from k_{min} to k_{max} . For $|k| < \Theta_{D\ell}/v$:

$$\mathcal{C}_{\ell}^{(1)} = \begin{cases} [k, -(1 - 2c_{\ell}/v)k] & \text{for } k > 0, \\ [-(1 - 2c_{\ell}/v)k, k] & \text{for } k < 0. \end{cases} \quad (\text{A5})$$

For the contour $\mathcal{C}_{\ell}^{(2)}$ in the integral for $S_{k\ell}^{(2)}$:

$$\mathcal{C}_{\ell}^{(2)} = \begin{cases} [k + \Theta_{D\ell}/v, k] \cup [-(1 + 2c_{\ell}/v)k, -k - \Theta_{D\ell}/v] & \text{for } k > 0, \\ [k - \sqrt{4(c_{\ell}/v)^2 k^2 + (\Theta_{D\ell}/v)^2}, (1 + 2c_{\ell}/v)k] \cup [k, k - \Theta_{D\ell}/v] & \text{for } k < 0. \end{cases} \quad (\text{A6})$$

The $k > 0$ part of this solution corresponds to the darker shaded area in Fig. 9.

Keeping in mind the above results we rewrite the collision integral in the following form:

$$S_k = \sum_{\ell} S_{k\ell}, \quad (\text{A7})$$

$$S_{k\ell} = \mathcal{A}_{\ell} \int_{\mathcal{C}_{\ell}} \frac{dk'}{2\pi} \left| \frac{kk'(k - k')^2}{e^{(|k| - |k'|)/k_T} - 1} \right| (\xi_{k\ell})_x^2 \left\{ \frac{e^{|k|/k_T} - 1}{e^{|k'|/k_T} - 1} f_k^1 - \frac{e^{-|k'|/k_T} - 1}{e^{-|k|/k_T} - 1} f_{k'}^1 \right\}, \quad (\text{A8})$$

where

$$\mathcal{A}_{\ell} = \frac{V_0}{64\pi^3 m_i} \left(\frac{g_{sp}}{c_{\ell}} \right)^2, \quad (\text{A9})$$

$$\text{and} \quad k_T = T/v. \quad (\text{A10})$$

The contour \mathcal{C}_{ℓ} is the union $\mathcal{C}_{\ell}^{(1)} \cup \mathcal{C}_{\ell}^{(2)}$. For $|k| < \Theta_{D\ell}/v$ we must integrate between $\pm(|k| + \Theta_{D\ell}/v)$. For $|k| > \Theta_{D\ell}/v$ we must integrate between $k \pm \Theta_{D\ell}/v$ and between $-k \pm \sqrt{4(c_{\ell}/v)^2 k^2 + (\Theta_{D\ell}/v)^2}$. In both cases a window of the width $4c_{\ell}|k|/v$ centered around $k' = -k$ must be deleted from the integration interval. In Fig. 9 one can identify this window with the unshaded area around line OB .

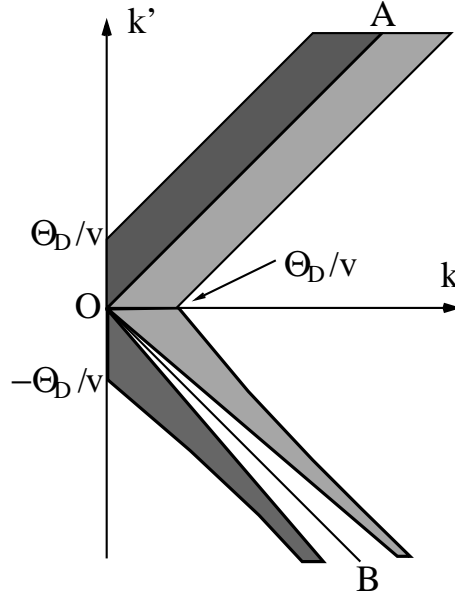


FIG. 9: This diagram shows the regions in the momentum space, allowed by the momentum and energy conservation, for the spin boson scattered from the state k to the state k' . The processes in which the original spin boson decays into another spin boson and emits the phonon are represented by the light gray area. For them $|k'| < |k|$ as dictated by the energy conservation. The dark gray area corresponds to the processes of phonon absorption by the spin boson. For them $|k'| > |k|$. Lines OA and OB are bisectors $k' = \pm k$.

We start by making the following observation. In general, the intervals \mathcal{C}_ℓ in (A8) differ for different polarizations $\ell = l, t$: the size of the gap around $k' = -k$ depends on the value of c_ℓ , so do $\Theta_{D\ell}/v$ which specify the outer limits of the integration intervals. However, we will show later that these variations in \mathcal{C}_ℓ do not change the integrals (A8) significantly. Therefore, it is convenient to introduce $\mathcal{C}_0 = \mathcal{C}_l \cap \mathcal{C}_t$ and $\delta\mathcal{C}_\ell = \mathcal{C}_\ell - \mathcal{C}_0$. Using this notation we write:

$$S_\ell = \int_{\mathcal{C}_\ell} \dots = \int_{\mathcal{C}_0} \dots + \int_{\delta\mathcal{C}_\ell} \dots \quad (\text{A11})$$

As it was mentioned the integrals over $\delta\mathcal{C}_\ell$ in the above expressions are small. Hence, it is permissible to integrate over \mathcal{C}_0 in both S_t and S_l . In such a situation the summation over polarization ℓ can be done easily since in both S_t and S_l only the product $\mathcal{A}_\ell(\xi_\ell)_x^2$ depends on polarization. Thus:

$$\tilde{\mathcal{A}} = \sum_\ell \mathcal{A}_\ell(\xi_\ell)_x^2 = \mathcal{A}_t, \quad (\text{A12})$$

where $\xi_{lx} = c_l|k - k'|/v||k| - |k'|$ and $\xi_{tx} = \sqrt{1 - (c_t|k - k'|/v||k| - |k'|)|^2}$. Therefore, the collision integral itself is equal to:

$$S_k = \tilde{\mathcal{A}} \int_{\mathcal{C}_0} \frac{dk'}{2\pi} \left| \frac{kk'(k - k')^2}{e^{(|k| - |k'|)/k_T} - 1} \right| \left\{ \frac{e^{|k|/k_T} - 1}{e^{|k'|/k_T} - 1} f_k^1 - \frac{e^{-|k'|/k_T} - 1}{e^{-|k|/k_T} - 1} f_{k'}^1 \right\}. \quad (\text{A13})$$

The first term of this integral can be calculated for small $|k|$:

$$\tilde{\mathcal{A}} f_k^1 \int_{\mathcal{C}_0} \frac{dk'}{2\pi} \left| \frac{kk'(k - k')^2}{e^{(|k| - |k'|)/k_T} - 1} \right| \frac{e^{|k|/k_T} - 1}{e^{|k'|/k_T} - 1} \approx \tilde{\mathcal{A}} f_k^1 \frac{k^2}{k_T} \int_{-\Theta_{D/v}}^{\Theta_{D/v}} \frac{dk'}{2\pi} \frac{|k'|^3}{2 \cosh(k'/k_T) - 2} = \frac{f_k^1}{\tau_{\text{sp}}(k)}, \quad (\text{A14})$$

which gives the spin-boson transport relaxation time:

$$\tau_{\text{sp}} = \begin{cases} v^3/\mathcal{A}T^3k^2 & \text{for } T \ll \tilde{\Theta}_D \\ v^3/\mathcal{A}\tilde{\Theta}_D^2Tk^2 & \text{for } T \gg \tilde{\Theta}_D \end{cases} \quad (\text{A15})$$

$$\text{with } \mathcal{A} = \frac{I_1(\infty)}{2\pi} \tilde{\mathcal{A}} \approx 2.3\tilde{\mathcal{A}}, \quad \tilde{\Theta}_D = \frac{\Theta_D}{\sqrt{I_1(\infty)}} \approx 0.25\Theta_D, \quad (\text{A16})$$

where $I_1(z)$ is defined in Eq. (31). One can see from Eq. (A14) that the dominant scattering process is the absorption of a phonon with the characteristic energy $\sim T$ as this energy range provides the major contribution to the integral.

If we neglect the second term of (A13) as well as the corrections to the collision integral coming from $\delta\mathcal{C}_\ell$ the function f_k^1 can be found right away. For example, if $T \ll \tilde{\Theta}_D$:

$$f_k^1 = \left\{ \frac{v^4}{\mathcal{A}T^4|k|} \frac{\partial}{\partial k} f_k^0(T) \right\} \partial_x T. \quad (\text{A17})$$

This is the expression for odd (in k) part of the spin boson distribution function. Using it we estimate the omitted term of (A13) and show that this term is small:

$$-\tilde{\mathcal{A}} \int_{c_0} \frac{dk'}{2\pi} \left| \frac{kk'(k-k')^2}{e^{(|k|-|k'|)/k_T} - 1} \right| \frac{e^{-|k'|/k_T} - 1}{e^{-|k|/k_T} - 1} f_{k'}^1 = -\tilde{\mathcal{A}} \int_{c_0} \frac{dk'}{2\pi} \left| \frac{kk'}{e^{(|k|-|k'|)/k_T} - 1} \right| [k^2 - 2kk' + k'^2] \frac{e^{-|k'|/k_T} - 1}{e^{-|k|/k_T} - 1} f_{k'}^1.$$

Of three terms in the square brackets only the second gives non-vanishing contribution to the integral. Two others do not contribute because they are even in k' and function $f_{k'}^1$ is odd. Therefore:

$$-\tilde{\mathcal{A}} \int_{c_0} \frac{dk'}{2\pi} \left| \frac{kk'(k-k')^2}{e^{(|k|-|k'|)/k_T} - 1} \right| \frac{e^{-|k'|/k_T} - 1}{e^{-|k|/k_T} - 1} f_{k'}^1 \approx \frac{2k}{\alpha k_T^3} \partial_x T \int_{-\Theta/v}^{\Theta/v} \frac{dk'}{2\pi} k' \frac{\partial}{\partial k'} f_{k'}^0 \approx \left\{ \frac{2k}{\pi \alpha k_T^2} \log \frac{k_{min}}{k_c} \right\} \partial_x T, \quad (\text{A18})$$

where $k_{min} = \min\{k_T; \Theta_D/v\}$. Since the integral in (A18) diverges at small $|k'|$ we must introduce small cut-off parameter k_c . Such a cut-off is associated with the impurity scattering. It is equal to the momentum at which the impurity scattering rate becomes comparable with τ_{sp}^{-1} . For now it is enough to assume that k_c is not too small so we can neglect the logarithm in the above formula. The expression (A18) is to be compared with (A14). For $T \ll \tilde{\Theta}_D$:

$$\frac{f_k^1}{\tau_{sp}} \approx \frac{1}{k} \partial_x T \gg \left\{ \frac{2|k|}{\pi \alpha k_T^2} \log \frac{k_T}{k_c} \right\} \partial_x T \Leftrightarrow |k|^2 \ll k_T^2. \quad (\text{A19})$$

In other words, at low temperatures the second term of (A13) is small as long as $|k| \ll k_T$. The same is true for larger temperature ($T \gtrsim \tilde{\Theta}_D$) as well.

We also need to estimate the integrals over $\delta\mathcal{C}_\ell$ to demonstrate that they are small. First, let us consider the integral over $\delta\mathcal{C}_t$. This interval is localized near $k' = -k$:

$$\delta\mathcal{C}_t = [-(1 + 2c_l/v)k, -(1 + 2c_t/v)k] \cup [-(1 - 2c_t/v)k, -(1 - 2c_l/v)k]. \quad (\text{A20})$$

It is non-vanishing as long as $c_l > c_t$. It is necessary to perform the integral (A8) with $\ell = t$ over $\delta\mathcal{C}_t$:

$$\begin{aligned} \mathcal{A}_t \int_{\delta\mathcal{C}_t} \frac{dk'}{2\pi} \left| \frac{kk'(k-k')^2}{e^{(|k|-|k'|)/k_T} - 1} \right| (\xi_{kt})_x^2 \left\{ \frac{e^{|k|/k_T} - 1}{e^{|k'|/k_T} - 1} f_k^1 - \frac{e^{-|k'|/k_T} - 1}{e^{-|k|/k_T} - 1} f_{k'}^1 \right\} \\ \approx 4k^4 \mathcal{A}_t \{f_k^1 - f_{-k}^1\} \int_{\delta\mathcal{C}_t} \frac{dk'}{2\pi} \left(1 - \frac{c_t^2(k-k')^2}{v^2(|k|-|k'|)^2} \right) \left| \frac{1}{e^{(|k|-|k'|)/k_T} - 1} \right| \\ \approx \frac{2\mathcal{A}_t}{\pi} T k^4 \{f_k^1 - f_{-k}^1\} \int_{\delta\mathcal{C}_t} dk' \frac{v^2(|k|-|k'|)^2 - c_t^2(k-k')^2}{v^3||k|-|k'||^3}. \end{aligned} \quad (\text{A21})$$

The absolute value of the last expression can be bounded from above by the following:

$$\frac{\mathcal{A}_t}{4\pi c_t^3} T |k| |f_k^1 - f_{-k}^1| \int_{\delta\mathcal{C}_t} dk' (v^2(|k|-|k'|)^2 - c_t^2(k-k')^2) \approx \frac{4\mathcal{A}_t}{\pi} k_T k^4 |f_k^1 - f_{-k}^1| \left(\frac{1}{3} \frac{(c_l - c_t)^3}{c_t^3} + \frac{(c_l - c_t)^2}{c_t^2} \right) \quad (\text{A22})$$

The latter expression can be estimated as $\propto \mathcal{A}_t k_T k^4 |f_k^1|$. This quantity is smaller than (A14) for $|k| < k_T$ as long as $(k/k_T)^2 \ll 1$.

Second, we estimate the integral (A8) with $\ell = l$ over $\delta\mathcal{C}_l$:

$$\delta\mathcal{C}_l = [|k| + \Theta_{Dl}/v, |k| + \Theta_{Dt}/v] \cup [-|k| - \Theta_{Dt}/v, -|k| - \Theta_{Dl}/v]. \quad (\text{A23})$$

It is clear without extensive calculations that both terms of (A8) are proportional to $(\xi_{kl})_x^2 \approx (c/v)^2 \ll 1$. Thus, the integral over this interval does not contribute significantly to the collision integral of the spin bosons.

Therefore, we can conclude that for small T the collision integral can be approximated by the expression (A14).

APPENDIX B: IMPURITY SCATTERING

Now we can start evaluating the self-energy corrections to the spin boson Green's function. Our first step is the calculation of the Matsubara Green's function $\mathcal{D}(\tau)$. Since the perturbation is an exponential of the bosonic field $\tilde{\Phi}$ rather than a polynomial we present our calculation in details. The second order correction to the Green's function is given by:

$$\mathcal{D}_k(\tau) - \mathcal{D}_{0k}(\tau) \approx \frac{\delta J_{\text{imp}}^2}{2\pi^2} \int d\tau' d\tau'' \left\langle \left(b_k^\dagger(\tau) + b_{-k}(\tau) \right) e^{-i\sqrt{2\pi}\tilde{\Phi}(x_0, \tau')} e^{i\sqrt{2\pi}\tilde{\Phi}(x_0, \tau'')} \left(b_{k'}(0) + b_{-k'}^\dagger(0) \right) \right\rangle_{\text{connected}}. \quad (\text{B1})$$

The triangular brackets stand for the Matsubara time-ordered averaging, and x_0 is the impurity position. The bare boson Green's function

$$\mathcal{D}_{0k}(\tau) = \left\langle \left(b_k^\dagger(\tau) + b_{-k}(\tau) \right) \left(b_k(0) + b_{-k}^\dagger(0) \right) \right\rangle \quad (\text{B2})$$

is a Fourier transform of $\mathcal{D}_{0k, i\omega} = 2\omega_k / (\omega^2 + \omega_k^2)$. To calculate the expression in the triangular brackets in Eq. (B1) we must expand both exponents into Taylor series

$$\sum_{n,m} \frac{(-i\sqrt{2\pi})^n (i\sqrt{2\pi})^m}{n!m!} \left\langle \left(b_k^\dagger(\tau) + b_{-k}(\tau) \right) \tilde{\Phi}^n(x_0, \tau') \tilde{\Phi}^m(x_0, \tau'') \left(b_{k'}(0) + b_{-k'}^\dagger(0) \right) \right\rangle_{\text{connected}} \quad (\text{B3})$$

and apply Wick's theorem. The external operators b , b^\dagger can be contracted with fields $\tilde{\Phi}$ in four possible ways schematically shown in Fig. 2: (a) both external operators contracted with the monomial $\tilde{\Phi}^n(x_0, \tau')$, (b) both external operators contracted with the monomial $\tilde{\Phi}^m(x_0, \tau'')$, and (c) and (d) one external operator contracts with $\tilde{\Phi}^n(x_0, \tau')$ while another contracts with $\tilde{\Phi}^m(x_0, \tau'')$. Each contraction with the external operator acts on a monomial as a derivative with respect to the field $\tilde{\Phi}$ times $e^{ikx_0} \mathcal{D}_{0k} / \sqrt{L|k|}$ or $e^{-ik'x_0} \mathcal{D}_{0k'} / \sqrt{L|k'|}$. Effectively, contraction with an external operator is equivalent to differentiation with respect to $\tilde{\Phi}$ times some c -number. Because of that one can derive:

$$- \frac{\pi e^{i(k-k')x_0}}{L\sqrt{|kk'|}} \left\{ \mathcal{D}_{0k}(\tau') \mathcal{D}_{0k'}(\tau - \tau') + \mathcal{D}_{0k}(\tau'') \mathcal{D}_{0k'}(\tau - \tau'') - \mathcal{D}_{0k}(\tau') \mathcal{D}_{0k'}(\tau - \tau'') - \mathcal{D}_{0k}(\tau'') \mathcal{D}_{0k'}(\tau - \tau') \right\} \times \left\langle e^{-i\sqrt{2\pi}\tilde{\Phi}(x_0, \tau')} e^{i\sqrt{2\pi}\tilde{\Phi}(x_0, \tau'')} \right\rangle. \quad (\text{B4})$$

The first term in the curly brackets corresponds to the diagram (a) in Fig. 2, the second corresponds to the diagram (b) and so on. The gray bubbles in Fig. 2 correspond to $\langle e^{-i\sqrt{2\pi}\tilde{\Phi}(0, \tau')} e^{i\sqrt{2\pi}\tilde{\Phi}(0, \tau'')} \rangle$.

As we see from (B4), the impurity scattering explicitly violates the momentum conservation. It will be restored once we average over the impurity positions. Such impurity averaging leads to a simple change in the above expression: $\langle \langle e^{i(k-k')x_0} \dots \rangle \rangle_{\text{imp}} / L = n \delta_{k, k'} / a$, where n is the dimensionless impurity concentration. After that the impurity position x_0 is arbitrary and can be put to zero. This yields:

$$\mathcal{D}_k(\tau) - \mathcal{D}_{0k}(\tau) \approx \frac{1}{2} \int d\tau' d\tau'' \left\{ \mathcal{D}_{0k}(\tau - \tau') \mathcal{D}_{0k}(\tau'') + \mathcal{D}_{0k}(\tau - \tau'') \mathcal{D}_{0k}(\tau') - 2\mathcal{D}_{0k}(\tau - \tau'') \mathcal{D}_{0k}(\tau'') \right\} \Sigma_k(\tau' - \tau''), \quad (\text{B5})$$

$$\Sigma_k(\tau' - \tau'') = \frac{\delta J_{\text{imp}}^2 n}{a\pi|k|} \left\langle e^{-i\sqrt{2\pi}\tilde{\Phi}(0, \tau')} e^{i\sqrt{2\pi}\tilde{\Phi}(0, \tau'')} \right\rangle. \quad (\text{B6})$$

With the help of the standard formula for free bosonic field:

$$\langle e^{\alpha\tilde{\Phi}(x, \tau)} e^{-\alpha\tilde{\Phi}(x', \tau')} \rangle = e^{\alpha^2 \langle (\tilde{\Phi}(x, \tau) - \tilde{\Phi}(x', \tau'))^2 \rangle / 2} \quad (\text{B7})$$

the above equation can be rewritten in the ω -space as:

$$\mathcal{D}_{k, i\omega} - \mathcal{D}_{0k, i\omega} \approx \mathcal{D}_{0k, i\omega}^2 \Sigma_{k, i\omega}, \quad (\text{B8})$$

$$\Sigma_{k, i\omega} = \frac{\delta J_{\text{imp}}^2 n}{a\pi|k|} \int d\tau (e^{i\omega\tau} - 1) e^{-\pi \langle (\tilde{\Phi}(0, \tau) - \tilde{\Phi}(0, 0))^2 \rangle}. \quad (\text{B9})$$

The average of the bosonic fields can be evaluated as follows

$$g(\tau) = -\left\langle \left(\tilde{\Phi}(0, \tau) - \tilde{\Phi}(0, 0) \right)^2 \right\rangle = 2 \left\langle \tilde{\Phi}(0, \tau) \tilde{\Phi}(0, 0) \right\rangle - 2 \left\langle \tilde{\Phi}(0, 0)^2 \right\rangle \quad (\text{B10})$$

$$= 2vT \sum_{\omega \neq 0} \int_k \frac{e^{i\omega\tau} - 1}{\omega^2 + v^2 k^2} e^{-|k|a} = 2T \sum_{\omega \neq 0} (e^{i\omega\tau} - 1) I(\omega),$$

$$\text{with } I(\omega) = \frac{1}{\pi|\omega|} \int_0^{+\infty} \frac{e^{-a|\omega|x/v}}{1+x^2} dx. \quad (\text{B11})$$

It is possible to evaluate the integral $I(\omega)$ for small ($|\omega| \ll J \sim v/a$) and large ($|\omega| \gg J \sim v/a$) Matsubara frequency ω :

$$I(\omega) = \begin{cases} 1/2|\omega| & \text{for } |\omega| \ll J \\ v/\pi\omega^2 a & \text{for } |\omega| \gg J. \end{cases} \quad (\text{B12})$$

The fact that at large $|\omega|$ function $I(\omega)$ decays as an inverse ω^2 guarantees the convergence of the Matsubara sum. Unfortunately, it is impossible to continue our derivation analytically due to complex properties of I . To overcome this difficulty we utilize a trick. Rather than using the actual form of $I(\omega)$ we put a different function in its place:

$$\tilde{I}(\omega) = \frac{e^{-|\omega|/J}}{2|\omega|}. \quad (\text{B13})$$

Such a replacement preserves $|\omega| \ll J$ properties of the sum but radically improves convergence at large ω . Since we are not interested in the high energy ($\sim J$), short time ($\sim 1/J$) properties of Σ this procedure is justified. Now the Matsubara summation can be done and it leads to:

$$g(\tau) = T \sum_{\omega \neq 0} \frac{e^{i\omega\tau - |\omega|/J} - e^{-|\omega|/J}}{|\omega|} = \frac{1}{2\pi} \log \frac{(1 - e^{-2\pi T/J})^2}{(1 + e^{-4\pi T/J} - 2e^{-2\pi T/J} \cos 2\pi T\tau)}. \quad (\text{B14})$$

In deriving this formula we used the identity:

$$\sum_{\omega > 0} \frac{e^{\gamma\omega}}{\omega} = -\frac{1}{2\pi T} \log(1 - e^{2\pi T\gamma}), \quad (\text{B15})$$

which is correct for any complex γ , $\text{Re } \gamma < 0$. To prove this formula one can expand the logarithm in Taylor series with respect to powers of $e^{2\pi T\gamma}$.

Once $g(\tau)$ is calculated it must be substituted into (B9). Now we have to evaluate the Fourier integral:

$$F(\omega) = \int_0^\beta d\tau \frac{(e^{i\omega\tau} - 1)(1 - e^{-2\pi T/J})}{\sqrt{1 + e^{-4\pi T/J} - 2e^{-2\pi T/J} \cos 2\pi T\tau}}. \quad (\text{B16})$$

This integral can be transformed into an integral over a unit circle in the complex plane:

$$F = \frac{\sqrt{s}}{2\pi iT} \oint dz \frac{z^m - 1}{\sqrt{z((2+s)z - z^2 - 1)}}, \quad (\text{B17})$$

$$s = 4\pi^2 T^2 / J^2 \ll 1, \quad z = e^{2\pi iT\tau}, \quad m = \frac{\omega}{2\pi T} - \text{integer}. \quad (\text{B18})$$

The polynomial under the square root has three zeros: $z_0 = 0$ and $z_{1,2} \approx 1 \pm \sqrt{s}$. Our branch-cut consists of two components: the first component stretches from 0 to $1 - \sqrt{s}$, the second component stretches from $1 + \sqrt{s}$ to $+\infty$. Such a choice of the branch-cut ensures that the integration path, the unit circle, does not cross the branch-cut, see Fig. 10. It is possible now to change the integration path. The new integration path runs counterclockwise along the sides of $(0, 1 - \sqrt{s})$ component of the branch-cut. In turn, this integral can be transformed into an integral over the real axis:

$$F = \frac{\sqrt{s}}{\pi T} \int_0^{1-\sqrt{s}} dx \frac{(x^m - 1)\sqrt{x}}{\sqrt{(x-1)^2 - sx}}. \quad (\text{B19})$$

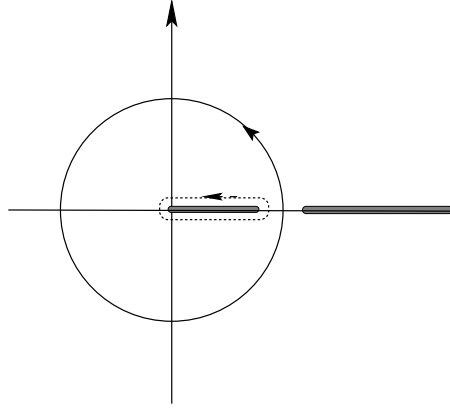


FIG. 10: The transformation of the integration path in the complex plane for Eq. (B17) is shown. The thick gray lines represent the branch cuts. The unit circle is transformed into a new contour circumventing one of the branch cuts. This new contour is shown by the dash line.

Finally, the Matsubara self-energy equals to

$$\Sigma_{k,i\omega} \approx \frac{\delta J_{\text{imp}}^2 n}{a\pi^2 T |k|} \sqrt{s} \int_0^1 dx \frac{(x^m - 1)\sqrt{x}}{x - 1}. \quad (\text{B20})$$

To obtain the retarded self-energy Σ^R the analytical continuation $m \rightarrow -i\omega/2\pi T$ must be done. For $\omega \ll T$ it gives:

$$\Sigma_{k,\omega}^R \approx -i \frac{\delta J_{\text{imp}}^2 n}{2aJ|k|T} \omega. \quad (\text{B21})$$

Once the self-energy is calculated one can find the retarded Green's function:

$$D_{k,\omega} = \frac{D_{0k,\omega}}{1 - D_{0k,\omega} \Sigma_{k,\omega}^R} = \frac{2\omega_k}{-\omega^2 + \omega_k^2 - 2\omega_k \Sigma_{k,\omega}^R} \quad (\text{B22})$$

and extract the lifetime from the position of the Green's function pole:

$$\omega^2 = \omega_k^2 - 2\omega_k \Sigma_{k,\omega}^R. \quad (\text{B23})$$

As a result the lifetime Γ is given by:

$$\Gamma = \frac{\Delta^2}{T}, \quad (\text{B24})$$

with the auxiliary parameter Δ is defined as

$$\Delta^2 \propto n \delta J_{\text{imp}}^2 \quad (\text{B25})$$

where n is the dimensionless impurity concentration.

¹ C. Hess, C. Baumann, U. Ammerahl, B. Büchner, F. Heidrich-Meisner, W. Brenig, and A. Revcolevschi, Phys. Rev. B **64**, 184305 (2001).

² C. Hess, U. Ammerahl, C. Baumann, B. Büchner, and A. Revcolevschi, Physica B **312**, 612 (2002).

³ C. Hess, H. ElHaes, B. Büchner, U. Ammerahl, M. Hückler,

and A. Revcolevschi, Phys. Rev. Lett. **93**, 027005 (2004).

⁴ A. V. Sologubenko, K. Giannó, H. R. Ott, U. Ammerahl, and A. Revcolevschi, Phys. Rev. Lett. **84**, 2714 (2000).

⁵ A. V. Sologubenko, K. Giannó, H. R. Ott, A. Vietkine, and A. Revcolevschi, Phys. Rev. B **64**, 054412 (2001).

⁶ A. V. Sologubenko, E. Felder, K. Giannó, H. R. Ott, A.

- Vietkine, and A. Revcolevschi, Phys. Rev. B **62**, R6108 (2000).
- ⁷ A.V. Sologubenko, H.R. Ott, G. Dhalenne, and A. Revcolevschi, Europhys. Lett. **62**, 540 (2003).
 - ⁸ B. C. Sales, M. D. Lumsden, S. E. Nagler, D. Mandrus, and R. Jin, Phys. Rev. Lett. **88**, 095901 (2002).
 - ⁹ R. Jin, Y. Onose, Y. Tokura, D. Mandrus, P. Dai, and B. C. Sales, Phys. Rev. Lett. **91**, 146601 (2003).
 - ¹⁰ B. Sales, R. Jin, and D. Mandrus, cond-mat/0401154.
 - ¹¹ K. Kudo, M. Yamazaki, T. Kawamata, T. Noji, Y. Koike, T. Nishizaki, and N. Kobayashi, J. Phys. Soc. Jpn. **73**, 2358 (2004).
 - ¹² J. Takeya, I. Tsukada, Y. Ando, T. Masuda, K. Uchinokura, I. Tanaka, R. S. Feigelson, and A. Kapitulnik, Phys. Rev. B **63**, 214407 (2001); J. Takeya, I. Tsukada, Y. Ando, T. Masuda, and K. Uchinokura, Phys. Rev. B **62**, R9260 (2000); A.M. Vasil'ev, V.V. Pryadun, D.I. Khomskii, G. Dhalenne, A. Revcolevschi, M. Isobe, and Y. Ueda, Phys. Rev. Lett. **81**, 1949 (1998).
 - ¹³ M. Hofmann, T. Lorenz, G. S. Uhrig, H. Kierspel, O. Zabara, A. Freimuth, H. Kageyama, and Y. Ueda, Phys. Rev. Lett. **87**, 047202 (2001).
 - ¹⁴ C. Hess, B. Büchner, U. Ammerahl, L. Colonescu, F. Heidrich-Meisner, W. Brenig, and A. Revcolevschi, Phys. Rev. Lett. **90**, 197002 (2003).
 - ¹⁵ Y. Nakamura, S. Uchida, T. Kimura, N. Motohira, K. Kishio, K. Kitazawa, T. Arima, and Y. Tokura, Physica C **185-189**, 1409 (1991).
 - ¹⁶ O. Baberski, A. Lang, O. Maldonado, M. Hücker, B. Büchner, and A. Freimuth, Europhys. Lett. **44**, 335 (1998).
 - ¹⁷ X. F. Sun, J. Takeya, S. Komiya, and Y. Ando, Phys. Rev. B **67**, 104503 (2003).
 - ¹⁸ M. Hofmann, T. Lorenz, K. Berggold, M. Grüninger, A. Freimuth, G. S. Uhrig, and E. Brück, Phys. Rev. B **67**, 184502 (2003).
 - ¹⁹ H. Sato, Progr. Theor. Phys. **13**, 119 (1955).
 - ²⁰ R. L. Douglass, Phys. Rev. **129**, 1132 (1963); D. C. McCollum, R. L. Wild, and J. Callaway, Phys. Rev. **136**, A426 (1964); D. Walton, J. E. Rives, and Q. Khalid, Phys. Rev. B **8**, 1210 (1973); D. Douthett and S. A. Fiedberg, Phys. Rev. **121**, 1662 (1961).
 - ²¹ D. J. Sanders and Walton, Phys. Rev. B **15**, 1489 (1977).
 - ²² H. N. De Lang, H. van Kempen, and P. Wyder, Phys. Rev. Lett. **39**, 467 (1977).
 - ²³ J. A. H. M. Buys and W. J. M. de Jonge, Phys. Rev. B **25**, 1322 (1982).
 - ²⁴ H. A. M. de Gronckel, W. J. M. de Jonge, Phys. Rev. B **37**, 9915 (1988).
 - ²⁵ S. Chakravarty, B. I. Halperin, and S. B. Nelson, Phys. Rev. B **39**, 2344 (1989).
 - ²⁶ H. J. Mikeska, J. Phys. C **11**, L29 (1978).
 - ²⁷ B. N. Narozhny, Phys. Rev. B **54**, 3311 (1996).
 - ²⁸ H. Castella, X. Zotos, and P. Prelovsek, Phys. Rev. Lett. **74**, 972 (1995).
 - ²⁹ X. Zotos, Phys. Rev. Lett. **82**, 1764 (1999).
 - ³⁰ X. Zotos and P. Prelovsek, in "Interacting Electrons in Low Dimensions", Kluwer Academic Publishers, 2003.
 - ³¹ J. V. Alvarez and C. Gros, Phys. Rev. Lett. **89**, 156603 (2002).
 - ³² F. Heidrich-Meisner, A. Honecker, D. C. Cabra, and W. Brenig, Phys. Rev. B **66**, R140406 (2002).
 - ³³ J. V. Alvarez and C. Gros, Phys. Rev. B **66**, 094403 (2002).
 - ³⁴ K. Saito, Phys. Rev. B **67**, 064410 (2003).
 - ³⁵ K. Saito and S. Miyashita, J. Phys. Soc. Jpn. **71**, 2485 (2002).
 - ³⁶ E. Orignac, R. Chitra, and R. Citro, Phys. Rev. B **67**, 134426 (2003).
 - ³⁷ E. Shimshoni, N. Andrei, and A. Rosch, Phys. Rev. B **68**, 104401 (2003).
 - ³⁸ N. Andrei, E. Shimshoni, and A. Rosch, cond-mat/0307578.
 - ³⁹ Some of these results were briefly reported previously in: A. V. Rozhkov and A. L. Chernyshev, Phys. Rev. Lett. **94**, 087201 (2005).
 - ⁴⁰ A. O. Gogolin, A. A. Nersesyan, and A. M. Tsvelik, *Bosonization and Strongly Correlated Systems*, (Cambridge University Press, 1998).
 - ⁴¹ D. C. Johnston, in *Handbook of Magnetic Materials*, vol. 10, (ed. by K. H. J. Buschow, Elsevier Science, North Holland, 1997).
 - ⁴² A. Junod, in *Physical Properties of High Temperature Superconductors II*, (ed. by D. M. Ginzberg, World Scientific Publ. Co., Singapore 1990).
 - ⁴³ J. M. Ziman, *Electrons and Phonons*, (Clarendon Press, Oxford, 1960).
 - ⁴⁴ G. D. Mahan, *Many-Particle Physics*, Third Edition (Kluwer Academic and Plenum, New York, 2000).
 - ⁴⁵ R. Berman, *Thermal conduction in solids*, (Clarendon Press, Oxford, 1976).
 - ⁴⁶ C. M. Bhandari and D. M. Rave, *Thermal conduction in semiconductors*, (Wiley Eastern Ltd, New Delhi, 1988).
 - ⁴⁷ I. Pomeranchuk, J. Phys. (USSR), **4** 249 (1941).
 - ⁴⁸ C. Herring, Phys. Rev. **95**, 954 (1954).
 - ⁴⁹ P. Erdős and S. B. Haley, Phys. Rev. **184**, 951 (1969).
 - ⁵⁰ C. L. Kane, M. P. A. Fisher, Phys. Rev. B **46**, 15233 (1992).
 - ⁵¹ Diagrams are drawn with JaxoDraw, see D. Binosi and L. Theussl, hep-ph/0309015.
 - ⁵² M. Oshikawa and I. Affleck, Phys. Rev. B **65**, 134410 (2002).
 - ⁵³ M. R. Li and E. Orignac, Europhys. Lett. **60**, 432 (2002).
 - ⁵⁴ L. Pintschovius, N. Pyka, W. Reichardt, A. Yu. Rumiantssev, N. L. Mitrofanov, A. S. Ivanov, G. Collin, and P. Bourges, Physica C **185-189**, 156 (1991).
 - ⁵⁵ P. Ribeiro, C. Hess, P. Reutler, G. Roth, and B. Büchner, J. Mag. Mag. Mat. **290-291**, 334 (2005).
 - ⁵⁶ Further clarification of this issue is planned for the future publication.
 - ⁵⁷ A discussion of the spin-phonon scattering in the spin-ladder materials has been given in C. Hess, C. Baumann, and B. Büchner, J. Mag. Mag. Mat. **290-291**, 322 (2005).